sustainability

MDPI

Review

An Overview of Sustainable Desalination with Freezing Crystallization: Current Development, Future Challenges, and Prospects

Senyao Zhao [1], Rongjie Zhu [2], Jiatong Song [1,*] and Han Yuan [1,*]

[1] Marine Engineering, College of Engineering, Ocean University of China, Qingdao 266100, China; zsy5565@stu.ouc.edu.cn
[2] Tandon School of Engineering, New York University, New York, NY 11201, USA; rz2892@nyu.edu
* Correspondence: songjiatong@ouc.edu.cn (J.S.); hanyuan@ouc.edu.cn (H.Y.)

Abstract: As global demand for freshwater grows, seawater desalination has become one of the most promising methods for obtaining freshwater. Many coastal nations have included it in their sustainable development plans and are actively advancing related technologies. Compared with traditional desalination methods, such as distillation and membrane-based desalination, seawater freezing desalination offers the benefit of producing large amounts of freshwater at lower costs. This study provides an overview of the main methods and principles of seawater freezing desalination and summarizes the latest research progress. This paper also discusses experimental and simulation studies of different principles. Current research shows that both direct and indirect seawater freezing desalination technologies have become relatively mature, laying a foundation for practical applications. Hydrate-based desalination, eutectic freezing technology, and vacuum freezing technology offer cost-reduction benefits, but existing technologies have limitations, making these areas hot topics in research. Additionally, this paper discusses the experimental progress and simulation methods associated with this, elaborates upon, and analyzes the freezing crystallization process and desalination efficiency from the perspective of the bottom layer of crystal growth, offering valuable insights for future research. It concludes by summarizing and predicting the development of these technologies, emphasizing their great potential due to their low-cost and sustainable features.

Keywords: seawater; freeze desalination; crystal growth; experiment research; numerical simulation

Citation: Zhao, S.; Zhu, R.; Song, J.; Yuan, H. An Overview of Sustainable Desalination with Freezing Crystallization: Current Development, Future Challenges, and Prospects. *Sustainability* **2024**, *16*, 10138. https://doi.org/10.3390/su162210138

Academic Editor: Mostafa Ghasemi Baboli

Received: 29 September 2024
Revised: 30 October 2024
Accepted: 13 November 2024
Published: 20 November 2024

1. Introduction

Driven by human daily activities and industrial development, global demand for freshwater resources has increased sharply. However, 97.5% of surface water is saline, and only 0.3% of freshwater is directly available for human use [1]. Population growth, accelerated industrialization, urbanization, and economic development have intensified this demand, exacerbating the global water crisis. As demand continues to rise while fresh-water supply remains limited, our planet is facing an increasingly severe freshwater shortage. Roughly half of the world's population currently experiences severe water scarcity for at least part of the year. One quarter of the world's population faces 'extremely high' levels of water stress [2]. According to the World Population Prospects 2024 Summary of Results released by the United Nations, the global population is expected to reach 10.3 billion by 2080 [3]. The large population will exacerbate the situation of insufficient freshwater resources.

Desalination is a technology that address freshwater shortages by treating seawater or brackish water to meet water supply needs. As shown in Figure 1, these technologies can be divided into the following two categories:

- Thermal methods, which mainly include multi-stage flash distillation (MSF), multi-effect distillation (MED), membrane distillation (MD), freeze desalination (FD), and hydrate desalination (HFD).
- Membrane methods, which mainly include reverse osmosis (RO), electrodialysis (ED), and nanofiltration (NF).

Thermal methods utilize the phase change of water through evaporation and subsequent condensation to achieve desalination [4]. Membrane methods employ the potential differences, such as pressure and concentration gradients, between two liquids to remove salt ions and other impurities from the solution, thereby achieving desalination [5].

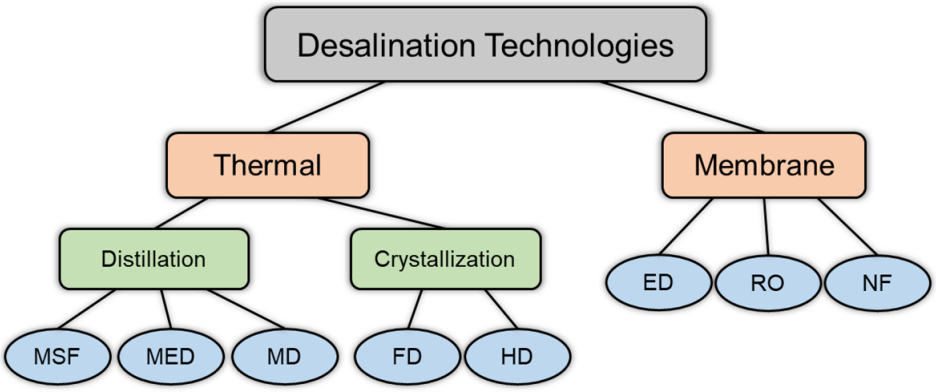

Figure 1. Classification of desalination technologies [6].

The latent heat of freezing for water is approximately 334.7 kJ/kg, which is about 15% of the latent heat of vaporization at 2255.3 kJ/kg [7]. The energy consumption of MSF is 18 kWh/m^3 [8], and this method requires operation at high temperatures, which can lead to scaling and corrosion. These issues not only affect system stability but also result in high construction and maintenance costs, hindering sustainable economic development [9]. Additionally, membrane fouling is a major issue in membrane desalination, as it not only increases maintenance costs but also shortens the lifespan of membranes. Moreover, to generate appropriate water fluxes during the desalination process, it is necessary to apply an osmotic pressure higher than that of the concentrate. Before the reverse osmosis stage, seawater needs to be pre-treated with microfiltration or ultrafiltration to remove dissolved substances and particulates from the raw seawater, thereby reducing membrane fouling and extending its lifespan [10]. However, this pre-treatment, further increases the cost of membrane desalination.

FD technology may effectively overcome many of the technical challenges faced by traditional desalination methods. This method separates the water in seawater from saltwater by freezing it. During the freezing process, water will preferentially crystallize and grow salt, removing salt from the solution. Freshwater is then extracted from the ice [11]. After these crystallized ice blocks are separated from the saltwater, they are washed and melted to obtain pure water. Figure 2 illustrates the principle of freezing desalination: as the temperature decreases, the saltwater cools to its freezing point, resulting in the formation of solid ice and a more concentrated brine solution.

Compared to the energy-intensive thermal methods and the expensive membrane methods, freeze desalination is a relatively eco-friendly and sustainable seawater desalination technology. This method is less prone to corrosion and scaling, allowing for lower operating and maintenance costs [12], while also eliminating the need for additional chemical agents, thus avoiding environmental pollution [13]. Additionally, FD can handle the high-concentration brine produced by methods such as MD and RO [14].

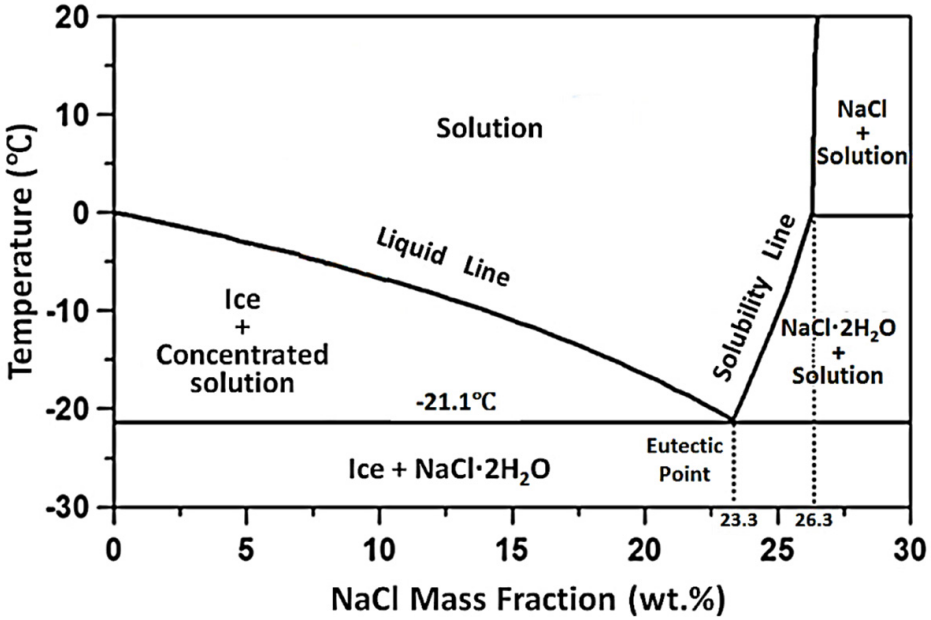

Figure 2. Phase equilibrium diagram of NaCl–H_2O binary solution.

Although seawater freezing desalination technology has many advantages, it has not yet been applied on a commercial scale. This is mainly due to a conservative attitude towards new technologies, with concerns that the process is mechanically too complex and lacks sufficient test data [15]. Additionally, the desalination mechanism in the freezing process is not yet fully understood, particularly its performance under different process parameters. A major challenge during the freezing process is that salts tend to remain trapped between ice crystals, forming high-concentration brine pockets [16], which necessitates additional Post-treatment or pre-treatment steps, thus increasing operational costs [17].

Although there are numerous experimental studies on FD, the scholarly domain lacks comprehensive evaluations of the latest developments in saltwater permeation, as observed in both experimental and computational research. To better understand the FD process, this paper will first provide a detailed explanation of the mechanism of seawater freezing desalination and summarize the most recent and representative developments across various desalination technologies. Based on this theoretical foundation, the paper will present the experimental and simulation progress of freezing desalination, focusing on the effects of experimental and simulation parameters (such as freezing temperature and salinity) on ice formation rates and salinity levels within the ice. Finally, the paper will discuss the challenges of freezing desalination and provide relevant recommendations.

2. Principles and Main Types of Seawater Freezing Desalination

FD is an application of freeze crystallization technology, in which dissolved salts are excluded during ice crystal formation, leading to the separation of ice and brine. However, in naturally frozen sea ice, due to the different crystallization temperatures of water and salt, salt tends to accumulate during freezing, forming brine pockets that get trapped within the sea ice [16]. To better understand the process of freezing desalination, Paul M. Williams [18] and his colleagues conducted the experiment presented in Figure 3b, where a solution containing methylene blue dye was placed in a metal beaker and slowly frozen. This process successfully separated the dye from the water. As also shown in Figure 3b, the edges of the ice block are almost pure water, while the center contains concentrated methylene blue solution, which can be drained off, leaving behind pure ice. However, Figure 3b also highlights the issue of small amounts of dye being trapped in the ice, resulting in a slight blue tint. Therefore, to obtain purer water, the ice needs to be washed to remove any residual dye before it is melted to produce freshwater. This simple experiment demonstrates the three main steps of the freeze separation process: lowering

the temperature to form ice, separating the ice from the brine, and melting the ice. Figure 3a shows the current main-stream freezing desalination process. First, seawater is introduced into a crystallizer to initiate the crystallization process. All types of freezing processes are defined by the form of freezing that occurs during crystallization. Once ice crystals form, the ice slurry is transferred to a separator, where the ice crystals and brine are separated. This apparatus usually takes the form of pressing, gravity drainage, centrifuges, filters, or washing columns [19]. Typically, this apparatus also serves as a washing device, where fresh water is used to wash the ice crystals to remove entrained brine. Finally, the ice crystals enter the melting unit, where freshwater is obtained after melting.

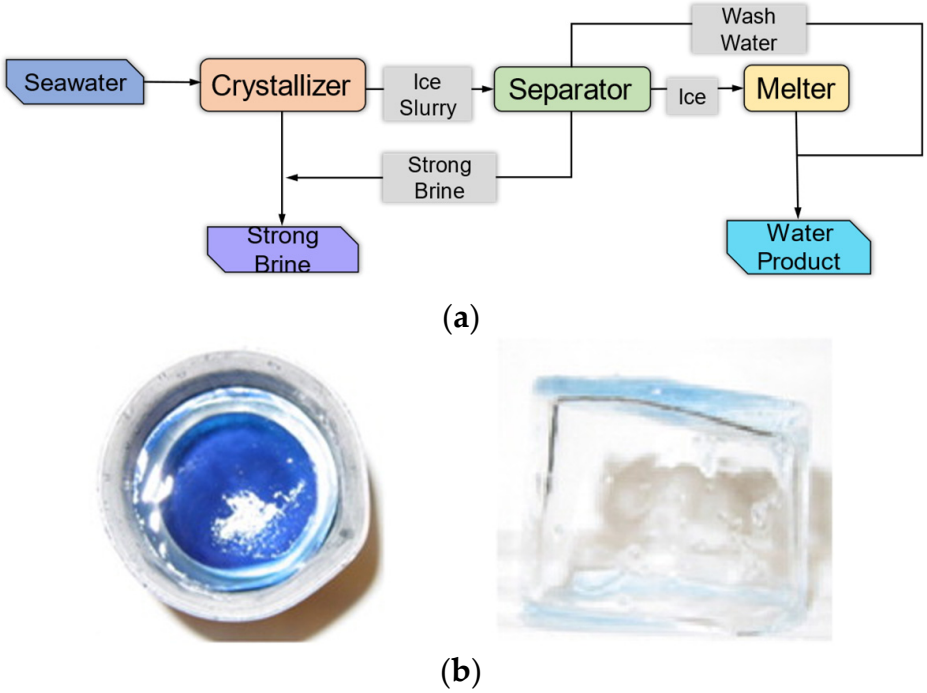

Figure 3. Illustration of freeze separation: (**a**) block flow diagram of basic freeze separation process; (**b**) experimental method for methylene blue dye [18].

The processes of freeze crystallization can be sorted into five separate groups, differentiated by the freezing conditions and techniques implemented within the crystallizer: (1) direct FD [20]; (2) hydrate FD [21]; (3) indirect FD [22]; (4) eutectic FD [23]; and (5) vacuum FD, each differentiated by their operating conditions. In seawater desalination, direct FD involves transferring cooling energy through direct contact between the refrigerant and the seawater. In contrast, indirect FD uses a thermally conductive solid surface to separate the refrigerant from the seawater. The cooling energy is transferred to the seawater via this surface, which is cooled by the circulating refrigerant. In both methods, the temperature remains above the eutectic point. However, if the cooling temperature is reduced to the eutectic point during the freezing process, eutectic freezing occurs [24]. Under these circumstances, the formation of salt crystals and ice occurs together, with separation achievable through gravitational forces. Moreover, vacuum freeze desalination (VFD) functions in an environment of elevated vacuum pressure. In this technique, the swift vaporization of a portion of the water removes considerable heat from the mixture, inducing a chilling effect that prompts the leftover water to turn into ice. Additionally, the water vapor that has evaporated can be recaptured and condensed back into drinkable water [25].

2.1. Direct FD

In this freezing desalination method, an insoluble liquid hydrocarbon refrigerant (such as butane) is introduced into the saline solution and comes into direct contact with the saltwater. Under low-pressure conditions, the refrigerant evaporates and vaporizes, rapidly absorbing a large amount of heat from the saltwater, causing the water molecules to nucleate and freeze. A schematic of the freezing desalination process is shown in Figure 4a. The resulting ice slurry then undergoes separation, washing, and melting steps to produce fresh water. The refrigerant vapor is compressed and condensed back to a high-pressure state, restarting the cycle. Meanwhile, the separated brine is used to pre-cool the incoming seawater, allowing for partial heat recovery.

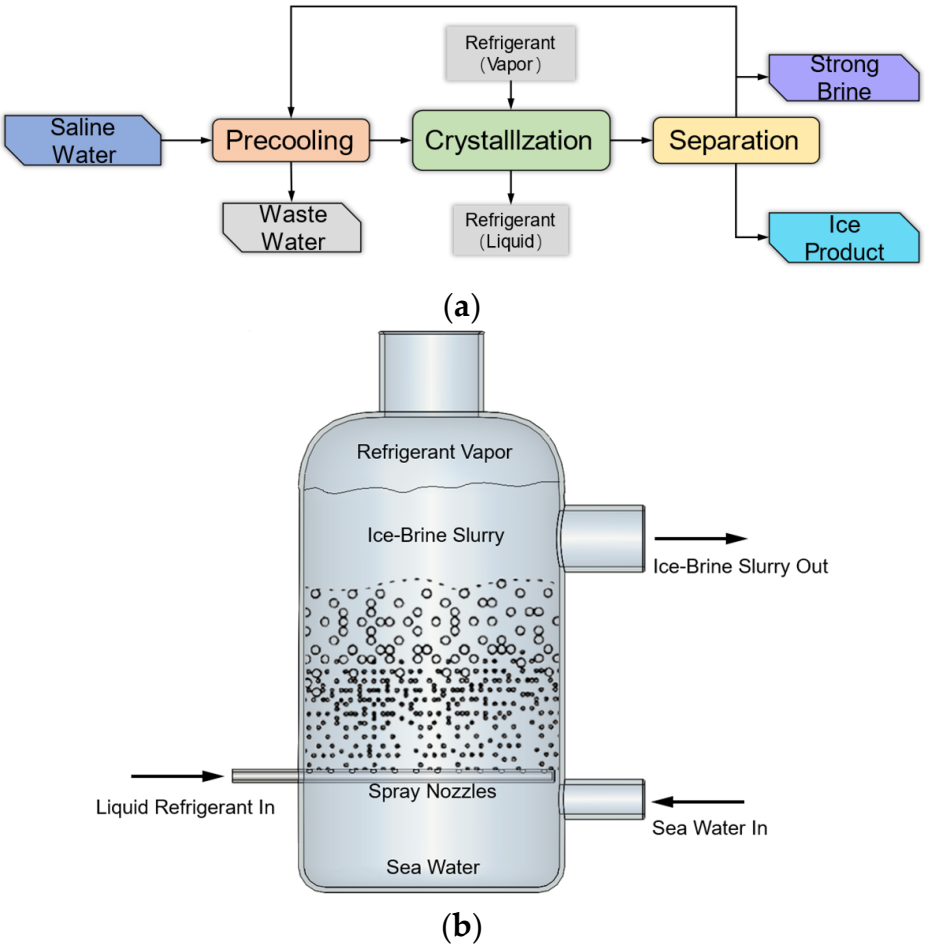

Figure 4. (**a**) Illustration of direct FD process chart; (**b**) schematic diagram of crystallizer [26].

The benefit of direct freeze desalination (FD) is its high efficiency in producing freshwater, stemming from the direct contact between saltwater solution and refrigerant, allowing for rapid transfer of cold energy [27]. Direct FD is considered the most effective method of freeze desalination [28,29], commonly utilizing non-soluble refrigerants like butane and freon, which vaporize upon contact with seawater [30], drawing out substantial latent heat and forming ice crystals. The refrigerants typically have boiling points below −4 °C and their evaporation pressures are relatively low, under 2.8 atmospheres. Additionally, refrigerants are non-toxic and exhibit relatively stable physicochemical properties in seawater, making it difficult to form hydrates with seawater. Nevertheless, a primary disadvantage of direct FD is that the refrigerant may not fully evaporate, leaving some residue in the ice, which can affect the safety of the produced drinking water [31]. Table 1 summarizes the key research findings on direct FD.

Table 1. State of the art in direct FD.

Reference	Methodology	Performance
M. Landau, A. Martindale [20]	Using butane as the refrigerant, the experiment tested the freezing performance of a stirred tank crystallizer, a segmented crystallizer, and a drainage tube crystallizer	Increasing the stirring rate and saline retention time improved the ice quality and reduced salt content, indicating that turbulence positively affects the ice crystal growth process.
Xie, zhang, liu, lv [32]	The jacketed structure, bottom 45-degree inclined nozzle arrangement, and air flotation technology were used to optimize the direct contact heat transfer process between the refrigerant and seawater.	At an initial refrigerant temperature of −60 °C and an ice mass fraction of 0.23–0.34, the ice maker achieved a volumetric heat transfer coefficient reduction from 92.5 to 81.9 $kW/m^3 \cdot °C$, achieving the optimal balance for the seawater freezing desalination process and efficient utilization of LNG cold energy.
Liu, ming, wu, richter, fang [33]	A spray freezing desalination system based on a natural ventilation tower was developed, utilizing large-area heat and mass transfer between cold air and sprayed water droplets to improve freezing efficiency.	Under an ambient temperature of −26 °C and with 2 mm water droplets, the system could produce 27.7 kg of freshwater per second.
Jiang, cao, fei, zhao [34]	Two wastewater treatment devices based on freeze separation were developed using an air-cooling device and a direct-contact cooling device.	When the solution concentration was 0.5 g/L, both freezing methods achieved over 90% removal of inorganic salts, with the copper contact cooling device showing the best performance in energy efficiency.
Mehdi, Amirsaman, Hossein [35]	A seawater freezing desalination system that directly utilizes LNG cold energy was developed, and a multi-objective optimization study was conducted to find the best combination of design variables to achieve maximum ice mass and minimum salinity.	The optimal LNG temperature was −47.5 °C, and under a Reynolds number below 16,000, the system could meet potable water standards after a three-stage freezing process.

2.2. Indirect FD

In contrast to direct FD, indirect FD involves the seawater and refrigerant not coming into direct contact, with a cold barrier surface separating the two, and with the solution's heat being transferred to the refrigerant through the wall, as shown in Figure 5. This method is mainly divided into two categories: suspended freeze crystallization [36] and progressive freezing on a cold surface [37], as shown in Figure 6.

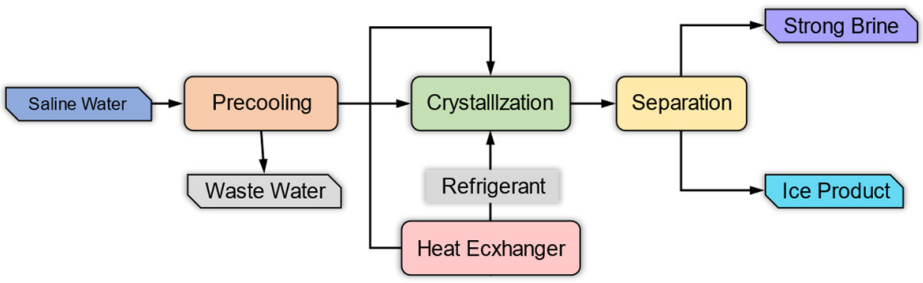

Figure 5. Illustration of indirect FD process.

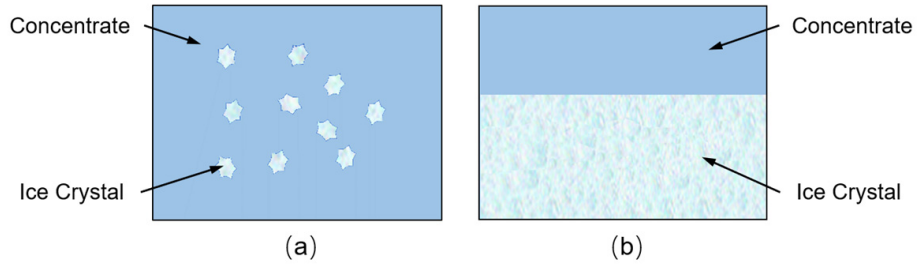

Figure 6. (**a**) Suspension freeze crystallization; (**b**) progressive freeze crystallization [38].

During the suspension crystallization process, the saltwater solution is circulated through a scraping surface heat exchanger at lower temperatures, encouraging the formation of tiny ice crystals (50 μm). Subsequently, the ice slurries are channeled back into the main vessel to facilitate crystal growth, and the ice is eventually isolated from the slurry through a filtration process.

Suspension crystallization typically cannot meet freshwater standards (≤0.1% salinity) because the ice crystals formed are small, and salts contaminate the surface of the ice crystals, with no uniform freezing direction provided. Additionally, studies show that the cost and challenges involved in using suspension methods for seawater desalination to meet freshwater standards are far greater than those required for progressive freezing [39]. Suspension freeze crystallization is a well-known process used in the food industry; however, in terms of cost and the simplicity of process and equipment, it is inefficient [36].

This is also the reason why current FD research focuses on progressive freezing desalination [40]. Initially, a monolayer of ice forms on the cooling surface, and as the freezing process continues, the ice layer's thickness gradually increases. Compared with suspension freeze crystallization, the ice crystals formed during the freezing of the ice layer are larger, which helps reduce the brine attached to the ice layer, thereby improving the desalination effect. Additionally, this method exploits the temperature differential between pure water crystallization and salt crystallization, resulting in greater freshwater yield with lower energy consumption [7].

The challenge of this method is that pure water crystallizes before the salt, causing the salt to accumulate and form "brine pockets" trapped in the ice crystals [41], leading to excessively high salt concentrations in the ice [42]. Therefore, Post-treatment techniques are required to purify seawater, mainly including water washing and centrifugation [43]. Due to these challenges, further improvements are necessary in the technology to reduce costs, increase freshwater production, and enhance water network interconnectivity.

Another option is to implement pre-treatment techniques instead of Post-treatment, with the key being to control crystallization conditions to suppress the formation of "brine pockets". Current research focuses primarily on spray freezing [44], vertical freezing [45], directional freezing [46] and axial freezing. These findings indicate that seawater freezing desalination is mainly influenced by the nucleation method, supercooling temperature, and cold flux, and that the latent heat released during crystallization affects the concentration and temperature gradients of the solution. However, the mechanism of brine pocket removal from ice crystals and the microscopic growth mechanisms remain unclear. Researchers are currently studying the inhibitory effects of pre-treatment techniques on brine pocket formation. Table 2 summarizes key research findings on indirect seawater desalination.

Table 2. State of the art in indirect FD.

Reference	Methodology	Performance
Osato, Liu, Shirai, Shigeru [38]	This paper designs a tubular ice system that uses a large cooling surface to promote the formation of single-crystal ice, simplifying the separation process of ice crystals from the mother liquor.	The results show that higher circulation rates and slower ice advancement speeds can significantly reduce the solute distribution coefficient and improve ice purity.
Yahui, Yudong, Jinyan, Xiao [47]	Batch experiments were conducted to study the effects of different freezing temperatures, initial concentrations, freezing rates, and total dissolved solids (TDS) on fluoride removal efficiency.	The results showed that the optimal temperature range is between −15 °C and −20 °C. In deionized water, the fluoride removal rate ranged between 75% and 85%.
Thouaïba, Claudia, Emilie, Denis [48]	The solid-liquid phase diagram of the water/acetone system was determined using differential scanning calorimetry (DSC) and the synthetic method.	The results indicated that the lowest impurity concentration was 3.92 g/L, requiring further Post-treatment steps to reduce the impurity content.
Jiang, cao, fei, zhao [34]	Two wastewater treatment devices based on freeze separation were developed using an air-cooling device and a direct-contact cooling device.	When the solution concentration was 0.5 g/L, both freezing methods achieved over 90% removal of inorganic salts, with the copper contact cooling device showing the best performance in energy efficiency.
Reza Kaviani, Hamidreza Shabgard, Aly Elhefny, Jie Cai, Ramkumar Parthasarathy [49]	A novel FD system utilizing an intermediate cooling liquid (ICL) is fabricated and used to desalinate brines.	At constant feed brine salinity, as the cooling temperature decreased the recovery ratio increased. At a fixed cooling temperature, the ice generation was greater for feed brine with smaller salinities.

2.3. Hydrate FD

Hydrate FD is considered quite similar to direct contact FD [50]. The desalination process, illustrated in Figure 7, involves the formation of water molecule cages around greenhouse gas molecules (e.g., CO_2, CH_4, C_2H_6, and SF_6) [51,52], resulting in natural gas hydrates under specific temperature and pressure conditions (TPC) [53]. During the process of seawater desalination and freshwater separation, these hydrates facilitate the removal of salts from the solution.

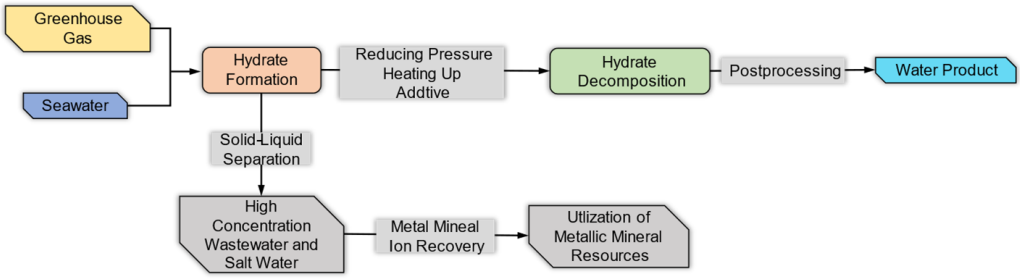

Figure 7. Freshwater separation process by the hydrate method.

CO_2 hydrates, in particular, have relatively milder formation conditions. While parameters such as induction time, generation rate, and volume may initially seem less favorable, they can be improved through the addition of thermal or kinetic enhancers and their synergistic effects. This makes CO_2 a viable guest gas for hydrate formation. By introducing gaseous or liquid hydrocarbons alongside CO_2 as formation gases [54], hydrates can form at temperatures above the freezing point. Notably, the formation of natural gas hydrates can raise the freezing point of the solution to as high as 12 °C [50], making this method highly effective under certain operating conditions.

The hydrate FD offers several unique advantages, including efficient greenhouse gas treatment and utilization, along with low-cost wastewater concentration, and freshwater production [55]. Additionally, the concentrated ion solution generated during this process can be used to extract valuable mineral resources [56].

The key to the hydrate FD process lies in the formation and decomposition of hydrate crystals, which occur under specific temperature and pressure conditions involving host and guest molecules. During the formation stage, the "hydrate cage" excludes salt ions and particulate pollutants [57]. The process is influenced by various factors such as the state of the guest molecules, the type of promoters used, the reaction system, and the apparatus. Once hydrate crystals are formed, Post-treatment methods such as filtration and centrifugation are employed to separate the crystals from the high-concentration impurity solution, resulting in pure hydrate crystals [58]. By subsequently adjusting the temperature and pressure conditions, the system is shifted out of hydrate phase equilibrium, enabling the separation of freshwater and recoverable guest molecules. Figure 8 illustrates the efficient implementation process of hydrate-based freshwater separation technology, while Table 3 summarizes key research findings related to the use of natural gas hydrates in seawater desalination.

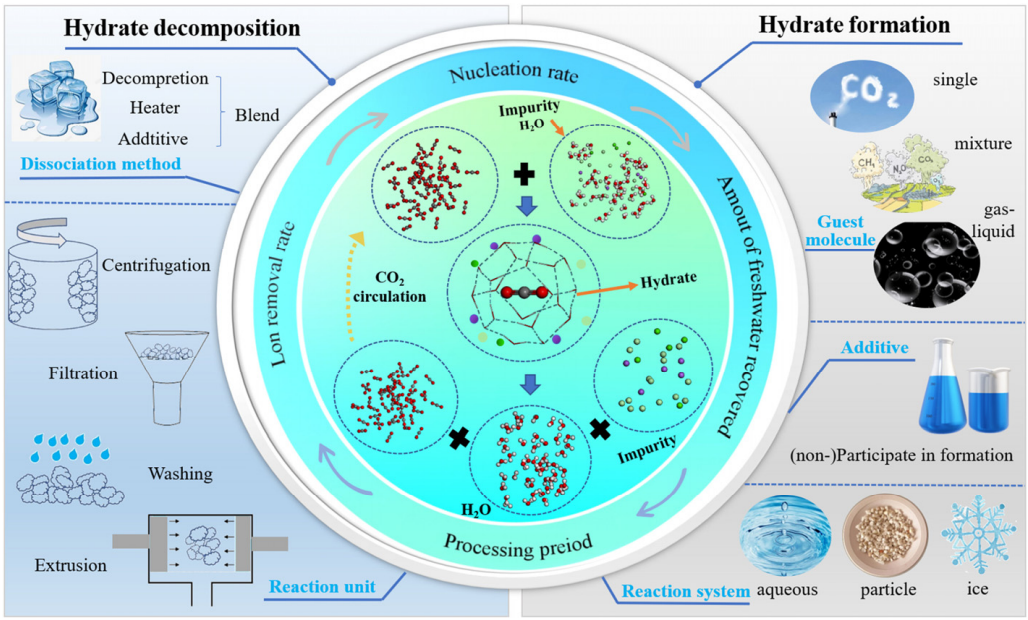

Figure 8. Efficient implementation process of freshwater separation technology by hydrate method [59].

Table 3. State of the art in hydrate FD.

Reference	Methodology	Performance
Hai, seong, changsu [60]	Using HFC134a as the hydrate-forming gas, a continuous hydrate formation-pressing-dissolution process was conducted, and Raman spectroscopy was used to analyze the hydrate structure.	In a single-stage hydrate process, 89% of dissolved minerals from seawater, approximately 80% of ions and total dissolved solids from hypersaline brine, and about 81% of pollutants from wastewater (Coca-Cola sample) were successfully removed.
Ponnivalavan, Abhishek, Zheng [61]	The cold energy produced during the regasification of liquefied natural gas (LNG) was used for hydrate formation and desalination.	Under a bed thickness of 1.9 cm and a hydrate formation time of 30 min, a water recovery rate of 34.85 ± 0.35% and a salt rejection rate of 87.5 ± 1.84% were achieved.

Table 3. *Cont.*

Reference	Methodology	Performance
Park, Hong, Lee, Kang [62]	A device was designed for the continuous production and compression of CO_2 hydrate particles, and Raman spectroscopy was used to analyze the hydrate structure.	The single-stage hydrate process effectively removed 72–80% of dissolved minerals, with the removal order being $K^+ > Na^+ > Mg^{2+} > B^{3+} > Ca^{2+}$.
Han, rhee, kang [63]	This study explored the seawater desalination process using cyclopentane hydrate formation and washing treatment technology.	Experimental results showed that approximately 63% of salt ions could be removed through single-stage hydrate formation and filtration, while subsequent washing treatment could further improve salt removal efficiency, reaching up to 90%.

2.4. Eutectic FD

Eutectic FD is a method that enables the simultaneous separation of ice and salt from saline wastewater under eutectic conditions, without the use of additional chemicals [64]. As seawater freezes, ice forms and floats, while the concentration of the remaining brine gradually increases. Once the seawater reaches its eutectic point, the salts begin to precipitate, forming salt crystals. Due to the density difference between the ice crystals and the salt crystals, they can be separated under the influence of gravity [65]. A simplified process flow diagram of the EFD process is shown in Figure 9.

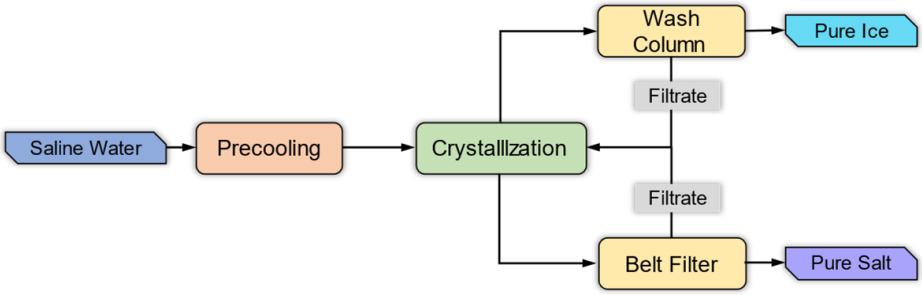

Figure 9. Illustration of eutectic FD process.

The EFD process starts with the brine solution being fed into a pre-cooler to lower its temperature, preparing it for the crystallization stage. The pre-cooled brine is then transferred into a crystallizer, where further cooling below the eutectic temperature results in the formation of both ice and salt crystals. The ice, which rises to the top of the crystallizer, is directed to a wash column where it undergoes purification through washing with cold water. This process effectively removes any remaining impurities, yielding pure ice as the final product [66].

As a freeze desalination method with low ice melting heat requirements, it demonstrates exceptionally high energy efficiency, making it highly advantageous for treating saline wastewater [65]. Life cycle assessments have shown that the EFD process significantly reduces both energy consumption and carbon footprint compared to traditional evaporative crystallization (EC) processes.

Additionally, the EFD process minimizes issues related to corrosion and scaling [18]. It also offers the benefit of recovering pure salt and water, which can be reused in industrial processes. This not only supports resource conservation but also reduces the overall cost of raw materials [67,68]. Table 4 provides a summary of key research findings related to EFD.

Table 4. State of the art in eutectic FD.

Reference	Methodology	Performance
A.E. Lewis, J. Nathoo, K. Thomsen, H.J. Kramer [69]	A eutectic freeze crystallization process was studied and designed for treating multi-component wastewater streams. Thermodynamic modeling and phase diagram tools were used to simulate the phase behavior of complex brine systems.	The first crystallization product was $Na_2SO_4 \cdot 10H_2O$ (3.5 °C), followed by ice (−5.25 °C), and finally $NaCl \cdot 2H_2O$ (−23.25 °C).
W. N. A. Mazli, S. Samsuri, N. A. Amran [70]	The article studied Progressive Freeze Concentration (PFC) and Eutectic Freeze Crystallization (EFC) technologies. Experiments were conducted using different stirring speeds, cooling times, and coolant temperatures to assess the efficiency of both methods.	The study found that in the PFC method, the optimal separation efficiency was achieved at a stirring speed of 300 RPM, a cooling time of 35 min, and a coolant temperature of −12 °C.
Debbie, Jemitias, Chivavava, Alison [71]	The occurrence of ice fouling development during the Eutectic Freeze Crystallization (EFC) process, where brine flows at low scraper velocities and experiences high supersaturation, was investigated. The impacts of the driving force for heat transfer, scraper rotation speed, and brine composition on the ice fouling formation time were analyzed.	The experiments showed that ice fouling formation is closely related to scraper speed, heat transfer driving force, and the type and concentration of impurities in the brine.
Mehdi, Roman, Jemitias, Joonas, Marjatta [72]	The research investigated the formation of ice crystals under conditions of minimal agitation and elevated levels of supersaturation within a jacketed, agitated eutectic freeze crystallization unit.	At low temperatures, ice fouling time is inversely proportional to temperature; at higher temperatures, stirring intensity significantly affects ice fouling time.

2.5. Vacuum FD

Vacuum FD employs a vacuum-assisted freezing mechanism to draw water vapor out of seawater, complemented by a vapor-compression process for vapor collection. At elevated vacuum pressures, a fraction of the seawater undergoes evaporation, and the evaporation removes the latent heat necessary to initiate the freezing process, effectively allowing the seawater to serve as the refrigerant, similar to direct FD. The vapor and ice formed during this process are collected, ultimately producing freshwater.

However, a primary obstacle to the broader adoption of vacuum freeze desalination (FD) is the substantial expense associated with the transportation of vapor at pressures below the triple point. This issue is further exacerbated by the lack of dependable ice formation management and the significant energy demands for the compression and collection of water vapor [7].

In their latest research, Cao and Wang [73] effectively showcased the concurrent freezing and vaporization of seawater, yielding pure water as both solid ice crystals and vapor under vacuum and triple-point circumstances. Their methodology incorporated the use of advanced nucleating agents, which facilitated zero thermal energy expenditure during the vacuum freezing stage.

In recent years, with the rapid advancement of LNG, the cold energy released during the LNG gasification process has garnered significant attention from scholars [74]. LNG regasification can generate approximately 840 kJ/kg of cryogenic energy. However, most of the cold energy released during the LNG regasification process is wasted. In order to maximize the efficient use of this cold energy, freeze desalination has become a suitable option for its utilization. Currently, there have been numerous experimental studies on

the combination of LNG with seawater freezing desalination. Table 5 summarizes the key research findings in this area.

Table 5. State of the art in LNG-FD.

Reference	Methodology	Performance
Attilio Antonelli [75]	A seawater desalination process based on LNG cold energy was proposed for the first time.	The study results showed that each ton of LNG can produce 3.2 tons of freshwater, and an LNG terminal processing 500 million cubic meters of natural gas per year can produce approximately 10,000 tons of freshwater daily.
Cao, Lu, Lin, Gu [76]	The FD process using LNG cold energy was developed and simulated using gPROMS software.	One kilogram of LNG cold energy is roughly equivalent to extracting 2 kg of freshwater.
Lin, Huang, Gu [77]	The system used R410A as a secondary refrigerant to cool seawater through heat exchange with LNG, utilizing a flake ice mechanism to produce ice.	The results showed that the system could achieve the designed freshwater production rate of 150 L/h, with a cold energy conversion efficiency of 2 kg freshwater/1 kg LNG. The system's single-stage freezing desalination rate was about 50%, indicating that multiple freezing cycles are needed to produce potable water.
Seong, Sang, Amadeu, Kun, Ju [78]	LNG cold energy was used as a cryogenic source for desalinating high-salinity water through gas hydrate formation.	HFC-134a achieved the fastest hydrate formation rate at a pressure of only 0.16 MPa.
Sang, Kyungtae [79]	A process design and economic analysis were conducted for gas hydrate-based combined power generation and seawater desalination using LNG cold energy.	he combined power generation cycle produced both pure water and electricity, with an energy consumption of −5.202 kWh, a simplified desalination cycle energy consumption of 0.566 kWh/ton of water, and a water production cost of $0.544.

2.6. Summary

This section reviews several major existing seawater desalination methods, including the widely used direct freezing desalination method and indirect freezing desalination method, as well as the hydrate freezing desalination method, eutectic freezing desalination method, and vacuum freezing desalination method, each of which show great potential for future development. The direct freezing method is highly efficient but has issues such as refrigerant residue and low ice crystal separation efficiency, limiting its application mainly to small-scale seawater desalination. The indirect freezing method currently has the widest application and strongest adaptability to production conditions. By utilizing existing cold sources such as liquefied natural gas (LNG), it enhances the overall energy efficiency, making it suitable for large-scale, high-efficiency, and long-term production scenarios. Hydrate freezing desalination is an efficient and environmentally friendly seawater desalination technology that achieves efficient utilization of greenhouse gases while enabling the concentration and reuse of wastewater. It features low energy consumption, high salt separation efficiency, and environmental friendliness. However, this technology is constrained by factors such as the state of guest molecules, the type of promoter, the reaction system, and desalination equipment. It is currently in the stages of theoretical and experimental research and limited to specific environmental applications. Eutectic freezing desalination has potential in wastewater treatment but is limited by high costs and complex equipment maintenance. Vacuum freezing desalination, on the other hand, offers advantages such as high-purity freshwater and low pollution emissions; however,

its technical complexity limits its broader application. The advantages of the desalination methods mentioned above are analyzed as shown in Figure 10.

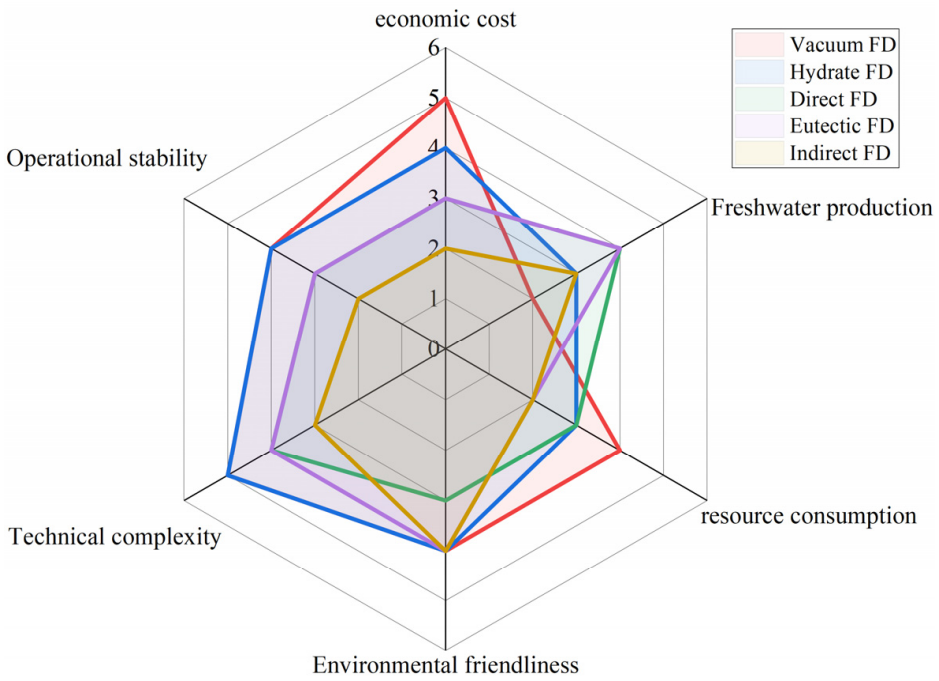

Figure 10. The characteristic analysis diagram of the desalination methods.

3. Progress in Experimental Study on Freeze Desalination

The basic types of freeze desalination systems were introduced in the previous section. This section will now focus on the experimental advancements in freezing desalination, grounded in the theory of freezing separation. The success of the FD process is largely dependent on the operating conditions during the crystallization phase. Critical factors influencing crystallization include initial solution concentration, refrigerant temperature, degree of supercooling, solution flow rate, and the presence of nuclei.

This article employs the following experimental parameters to assess the efficacy of various freeze crystallization techniques:

1. Ice crystal size;
2. Salt concentration in the produced ice;
3. Freshwater yield;
4. Growth rate of the ice crystal tip;
5. Desalination efficiency R and effective distribution constant K [80].

Desalination efficiency R and the effective distribution constant K are commonly used metrics to evaluate the performance of seawater desalination processes [6].

The desalination efficiency, denoted as R, is calculated by taking the difference between the initial salinity (C_0) and the salinity of the ice (C_{ice}), and dividing it by the initial salinity. It can be expressed by Equation (1) as follows:

$$R = \left(1 - \frac{C_{ice}}{C_0}\right) \times 100\% \quad (1)$$

The effective distribution constant K is defined as the ratio of the ice salinity C_{ice} to the salinity of the remaining concentrated solution C_L. It can be expressed by Equation (2) as follows:

$$K = \frac{C_{ice}}{C_L} \quad (2)$$

Numerous experimental studies have been conducted to improve desalination efficiency. This section provides a brief review of the research focused on enhancing desalination efficiency, including various freezing methods, identifying optimal operating parameters, and exploring Post-treatment and pre-treatment techniques. These efforts aim to enhance salt diffusion and mitigate salt retention during the desalination process.

As discussed in the previous section, most experimental work in seawater freezing desalination has employed indirect FD systems. Fujioka et al. [81] conducted a progressive freezing desalination experiment, illustrated in Figure 11, to investigate the effects of ice tip growth speed, stirrer rotation speed, and initial solution concentration on desalination performance. The study revealed that desalination efficiency improved with a decrease in ice tip growth speed and an increase in stirrer rotation speed. This aligns with findings in other literature, which suggest that slower cooling rates promote the formation of ice crystals with lower salinity [82,83]. Conversely, lower freezing temperatures lead to faster crystallization, which prevents salts from being expelled from the ice crystals in time, thereby reducing the desalination efficiency [84].

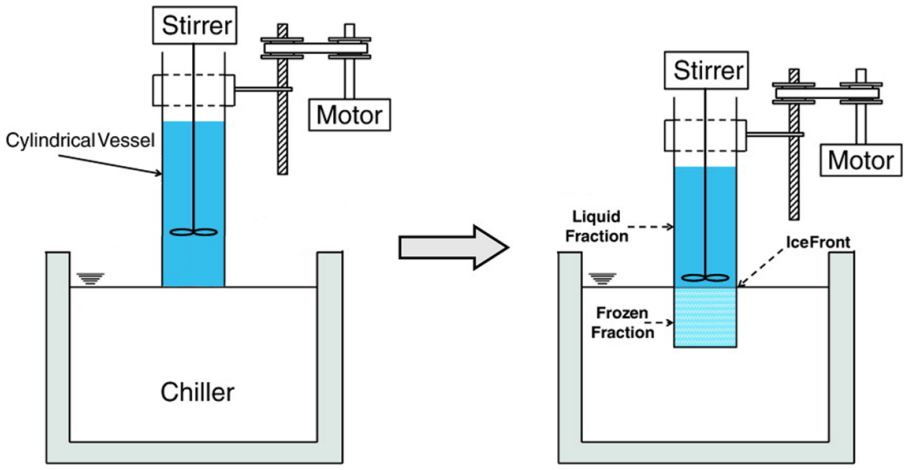

Figure 11. The laboratory equipment for progressive freeze desalination [81].

To address the issue of low desalination efficiency, researchers have proposed several methods. One key limitation is that a single freezing process cannot produce freshwater directly from seawater. Therefore, multiple desalination cycles involving freezing and melting of ice crystals can be performed until potable water standards are met. Jayakody et al. [85] used a combination of computational fluid dynamics simulations and experimental verification to demonstrate that gradual freezing and melting operations can reduce the salt content in ice, ultimately achieving desalination. Badawy et al. [86] experimentally examined the effects of crystallinity, the number of freeze-melt cycles, and gradual melting on total dissolved solids and salt removal efficiency, with results presented in Figure 12. After a single freeze-melt cycle, the TDS of the ice water was approximately 18,932 mg/L, significantly lower than the original seawater TDS of 40,916 mg/L. With multiple freeze-melt cycles, the TDS decreased further to 610 mg/L, which meets drinking water standards. In the gradual melting experiment, the TDS of the ice water dropped to 693 mg/L within 6 h. The study demonstrated that by controlling crystallinity and the number of freeze-melt cycles, seawater salt content can be effectively reduced without the need for chemical additives. Although multi-stage freezing desalination significantly improves efficiency, the increased complexity and costs associated with multiple freezing cycles raise the overall cost of producing potable water [87].

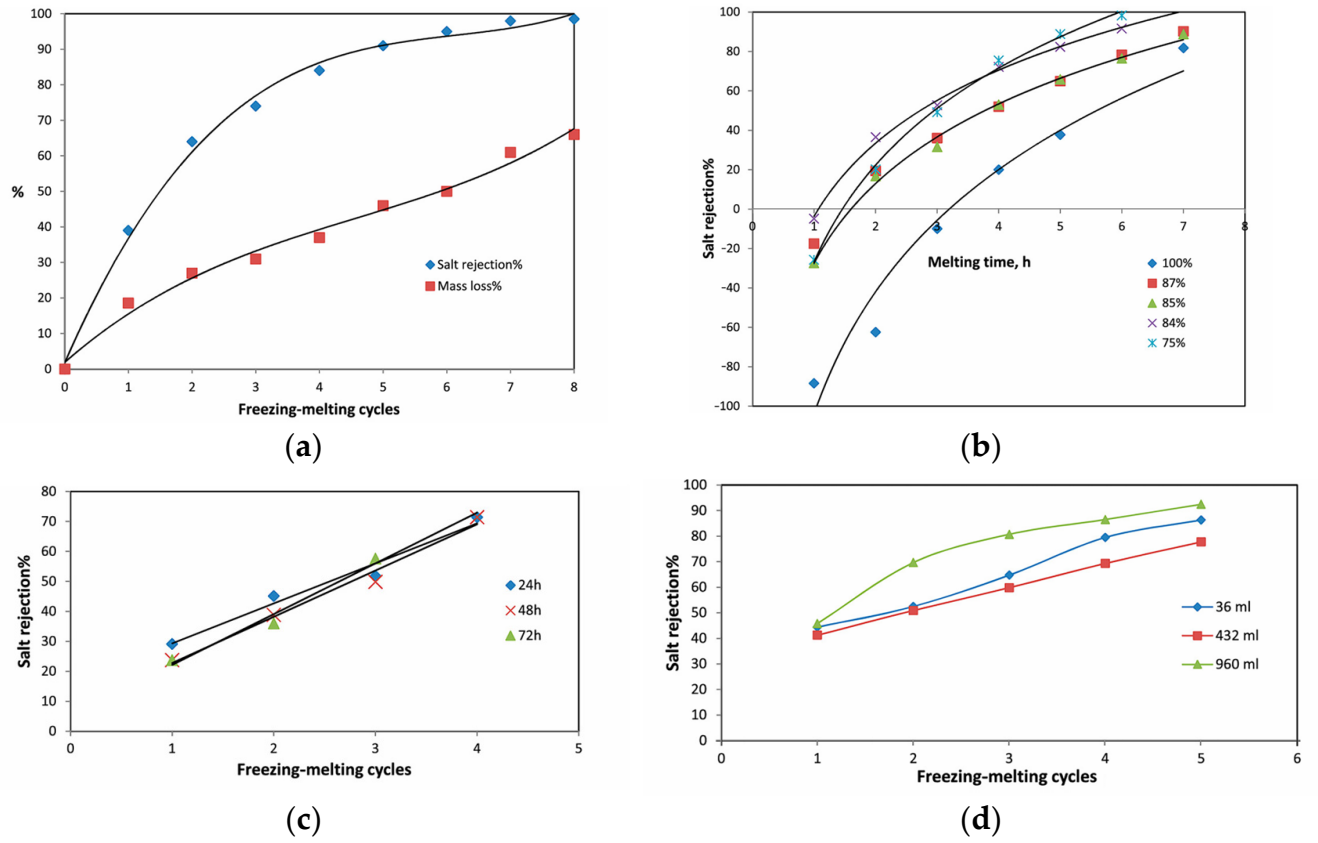

Figure 12. The influence of experimental parameters on desalination rate: (**a**) the influence of freezing melting cycles on desalination rate and freshwater loss; (**b**) melting time parameter; (**c**) the influence of freezing melting cycles on desalination rate and freshwater loss; (**d**) the influence of freezing melting cycles on desalination rate and freshwater loss [86].

Another method to improve desalination efficiency is to perform a post-treatment to the desalinated water after a single freezing desalination process. Post-treatment methods can reduce salt concentrations and increase freshwater yield, but the impact of Post-treatment processes on cost must also be balanced [88]. Erlbeck et al. [19] used high-pressure pressing of the frozen desalinated product to obtain high-purity freshwater, analyzing the effect of different pressures and holding times on desalination efficiency, Process schematic and effect are shown in Figure 13a. Chen et al. [89] achieved the freshwater salt content standard of 0.5% and obtained a 60% freshwater yield using Post-treatment methods, such as gravity filtration for 20 min or centrifugation for 1 min, Process schematic and effect are shown in Figure 13b. Additionally, after removing the surface salt from ice crystals through centrifugation, the freshwater salt content could reach the 0.05% drinking water standard. Similarly, washing ice crystals with seawater [88] or freshwater [61] is a simple and economical Post-treatment method that helps improve desalination efficiency, although the impracticality of using freshwater to produce more freshwater must be considered, Process schematic and effect are shown in Figure 13c.

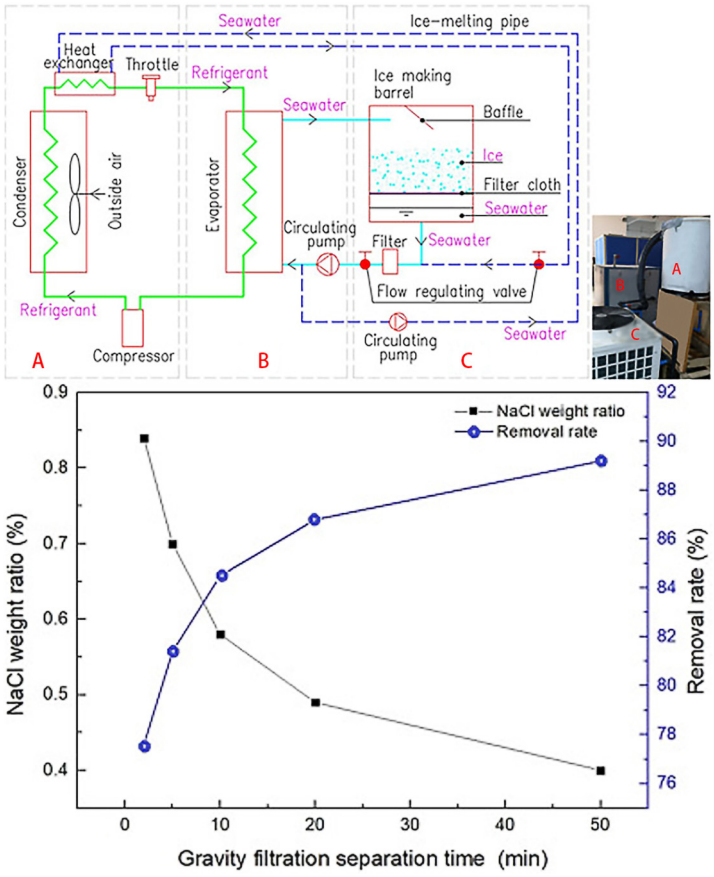

(**a**)

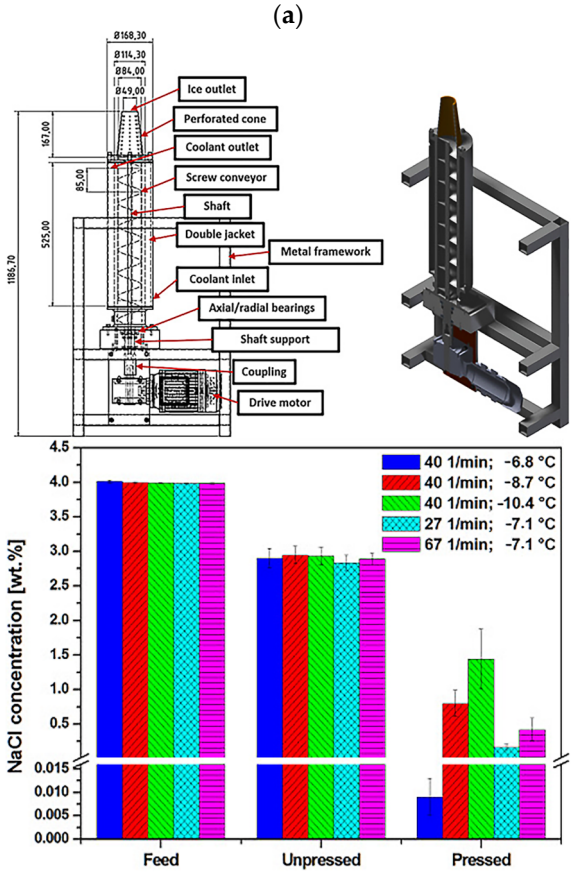

(**b**)

Figure 13. *Cont.*

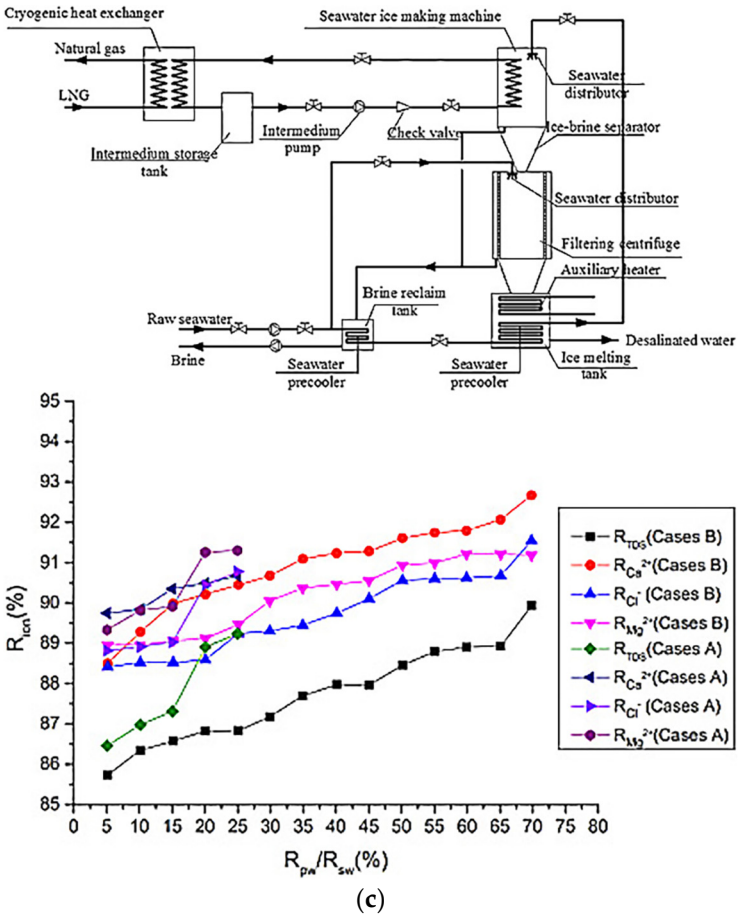

(**c**)

Figure 13. Process schematic and effect comparison diagram of different post-processing methods: (**a**) gravity and centrifugation [19]; (**b**) ice pressing [89]; (**c**) watering [88].

The treatment methods described above are referred to as Post-treatment methods, which use physical processes to improve desalination efficiency after freezing desalination and the formation of brine pockets. In contrast, methods applied before brine pocket formation are referred to as pre-treatment methods, which involve influencing the formation of brine pockets during the process of sea ice formation by applying physical means [90]. By altering external factors to influence crystallization conditions, pre-treatment methods affect the dendritic growth process of ice crystals. Currently, most scholars are conducting research aimed at fundamentally improving the quality of ice.

Song et al. [91] analyzed the crystallization process of seawater from the perspective of seawater flow, and designed experiments to compare ice crystal growth under different flow velocities. The diagram of experimental system is shown in Figure 14. The experimental results revealed that, compared to the ice crystal area in static seawater, the ice crystal area decreased by 21.8% at a flow velocity of 0.025 m/s, and by 25.3% at 0.05 m/s. The heat generated by seawater is a key factor affecting ice crystal growth. Additionally, Song et al. utilized heterogeneous particles to simulate ice crystal growth under heterogeneous nucleation conditions. The results indicated that, in the presence of heterogeneous particles, the ice crystal area was 10.8% larger than that under homogeneous nucleation conditions, with a difference of approximately 14.8% in the salt content of the ice crystals between the two conditions.

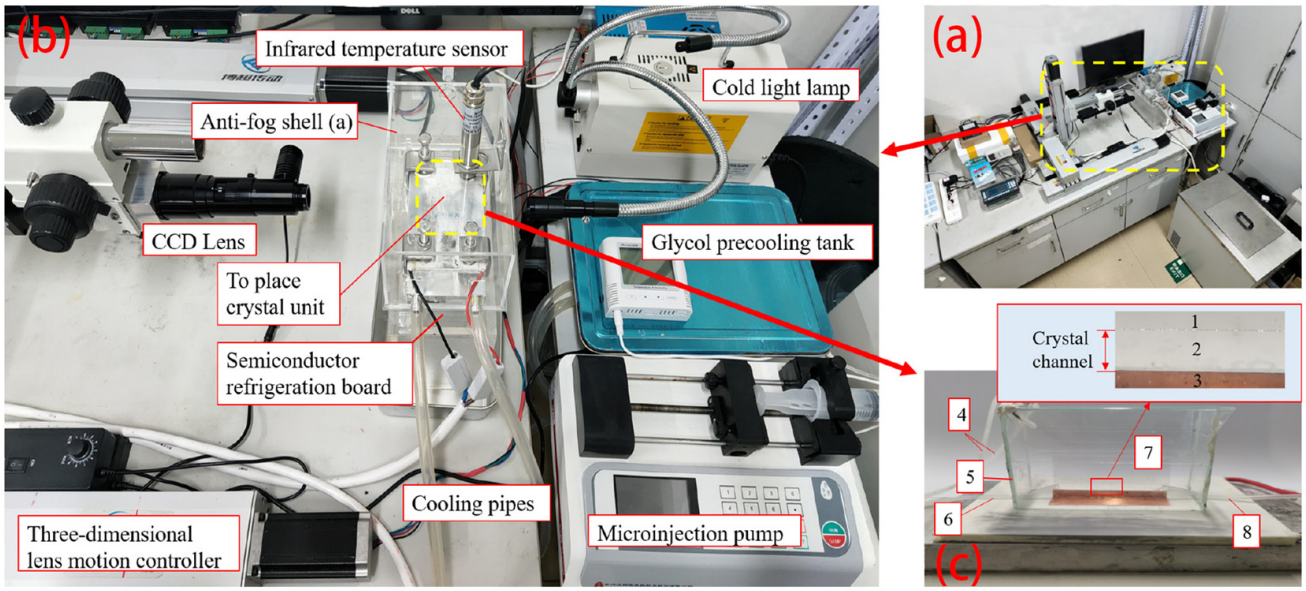

Figure 14. Diagram of experimental system: (**a**) Experiment setup; (**b**) Main equipment; (**c**) Crystal unit, 1, channel top (glass); 2, seawater; 3, copper base; 4, helium inlet/outlet; 5, anti-fog shell; 6, seawater inlet; 7, crystal observation unit; 8, seawater outlet [91].

Wang et al. [92] investigated the inhibitory effect of salt adsorption on the formation of salt pockets and conducted experiments on assisted adsorption during the directional growth of sea ice. The absorption freeze crystallization experimental system is shown in Figure 15. The results indicated that, under the influence of adsorption, the growth of salt pockets was inhibited, and the saltwater channels between adjacent ice crystals were significantly reduced. In the simulations and experiments, the area of the ice crystals increased by 6.08% and 11.79%, respectively.

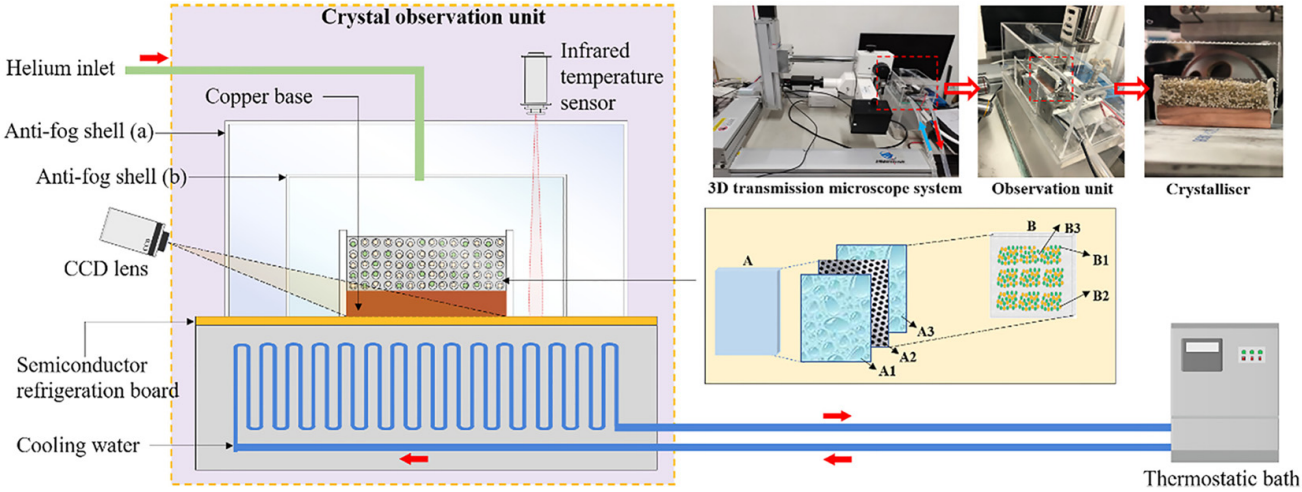

Figure 15. Schematic and pictures of absorption freeze crystallization experimental system. A: Sandwich crystallizer, A1: transparent glass (front), A2: stainless steel mesh plate, A3: transparent glass (back), B: adsorbent layer between A2 and A3, B1: cation exchange resin, B2: anion exchange resin, B3: seawater [92].

Some researchers have influenced the growth process of ice crystals by altering external environmental conditions. Song et al. [93] analyzed the effect of magnetic fields on crystal supercooling and the crystallization growth patterns of seawater. Under the influence of a direct current magnetic field, the ice crystal area increased by 103.9%, while the number of salt cells decreased by 13.05%. The application of an alternating current

magnetic field resulted in a 37.8% increase in the ice crystal area and a 17.0% improvement in overall seawater desalination rates, but it also increased the salt pocket formation by 11.6%. The stepped magnetic field did not affect the crystal area but increased the overall desalination rate by 14.3%. Zhang et al. [94] compared natural ice melting (NIM), oscillation ice melting (OIM), and ultrasound ice melting (UIM). OIM and UIM can promote ice desalination. When the OIM and UIM melt ice ratio reach 40% and 65%, the salt can meet agricultural irrigation water standard. The experimental platform for seawater crystallization is designed as shown in Figure 16. Yang et al. [95] applied microwaves in a combined process of centrifugal seawater desalination and gravity-induced desalination to study the effects of microwaves on ice production rate and crystallization time. The illustrating steps are shown in Figure 17. The findings indicated that microwave treatment significantly accelerated seawater desalination in both combined processes. By applying a two-minute microwave treatment, the desalination effect of gravity-induced desalination was improved compared to centrifugal seawater desalination. Using TDS and Cl^- concentrations as reference indicators, when the proportion of brine waste is greater than 54%, the quality of the ice products from gravity-induced desalination of seawater can meet drinking water standards.

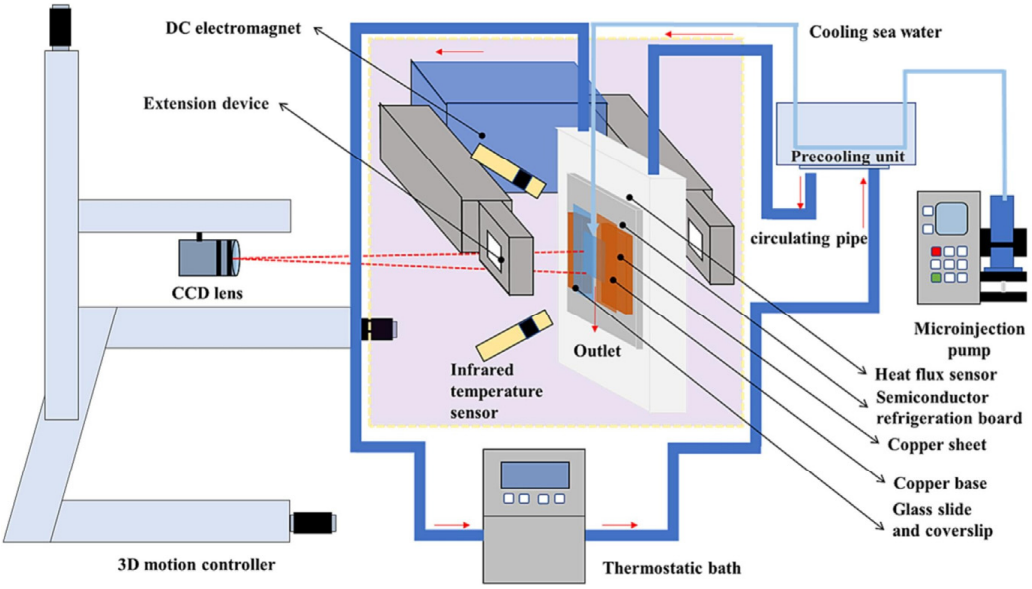

Figure 16. Design of an experimental platform for seawater crystallization under an external magnetic field [94].

Regarding the seawater freezing desalination method, this section summarizes the current state of experimental techniques in freezing desalination, focusing on comparative studies of experimental parameters, data processing, and salt diffusion effects that improve desalination rates. Experimental methods in academia have evolved from gradual experiments involving slow cooling to form low-salinity ice crystals to more advanced techniques such as freeze-thaw cycles, multi-stage freezing desalination, and high-pressure freezing desalination. Currently, most of these experimental techniques are limited to laboratory research. In optimizing technological pathways, the focus is on analyzing and improving inefficient processes to enhance desalination efficiency and reduce energy consumption. Furthermore, by introducing new materials in crystallization equipment that are corrosion-resistant, have good thermal conductivity, and high strength, the structural design of the equipment can be further optimized, improving performance and longevity, thereby providing more reliable support for the practical application of freezing desalination technology. Overall, freezing desalination experimental technology is still in continuous development, with multiple fields offering rich research opportunities and potential.

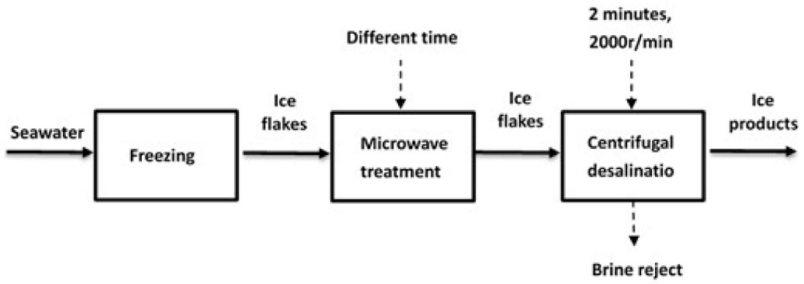

(a) FMCD (combined Freezing, Microwaving, Centrifugal Desalination) progress

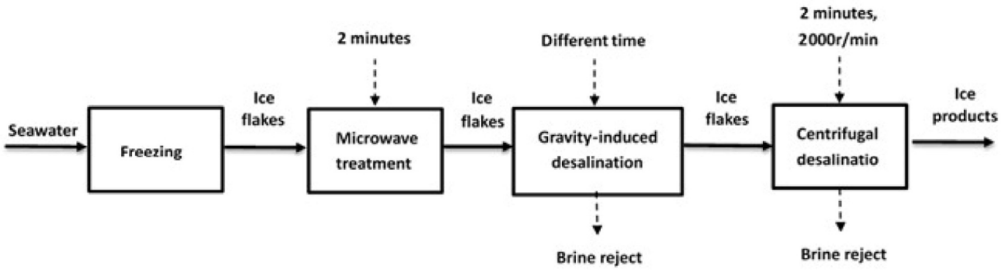

(b) FMGCD (combined Freezing, Microwaving, Gravity induced and Centrifugal Desalination) progress

Figure 17. Schematic diagram illustrating the steps for FMCD (**a**) and FMGCD process (**b**) [95].

4. Numerical Simulation Study on Freeze Desalination

Although significant progress has been made in experimental studies of freezing desalination, achieving better seawater desalination performance through controlling supercooling, nucleation, multi-stage freezing, and Post-treatment methods, it remains challenging to directly reveal the microscopic mechanisms of freezing desalination and their fundamental impact on desalination performance through experiments. Currently, research on seawater freezing desalination primarily focuses on the principles of ice formation and growth, as well as the mechanisms brine pocket formation. Experimental studies have certain limitations in investigating these principles and mechanisms. Numerical simulation, as a crucial research tool, can facilitate the study of cryogenic desalination mechanisms. It allows for the exploration of ice crystal growth and brine pocket formation at different scales [49,85,96].

Simulating seawater desalination through freezing is a complex multi-physics challenge involving the combined phenomena of heat and mass transfer. In both direct and indirect FD technologies, cold energy is transferred from the refrigerant to the solution, creating a temperature differential spurring the migration of salt. Heat exchange occurs via two primary processes: convection to the saline solution and conduction through the forming ice crystals. However, indirect freezing includes an additional step of conduction through a cold barrier between the saline solution and the refrigerant. In contrast, direct freezing involves the concurrent evaporation of the refrigerant as ice crystals form.

4.1. Computational Fluid Dynamics (CFD)

The computational fluid dynamics (CFD) software ANSYS Fluent has been used to simulate the indirect freezing seawater desalination process. Several numerical studies have examined the ice growth rate, control conditions, temperature distribution [97], heat transfer coefficients [98], unsteady heat transfer [99], and ice growth dynamics during continuous freezing [100].

The fundamental equations that regulate a typical indirect FD system for seawater are formulated in Equations (3)–(8). These are statements of the three conservation laws: mass, momentum, energy, and their derivatives such as the conservation of species, state equations, and additional functional relationships inferred from phase diagrams.

Liquid Fraction:

$$\phi = \begin{cases} 0 & T < T_{solidus} \\ \frac{T - T_{solidus}}{T_{liquidus} - T_{solidus}} & T_{solidus} < T < T_{liquidus} \\ 1 & T > T_{liquidus} \end{cases} \quad (3)$$

$$T_{solidus} = T_{melt} + \frac{m_S Y_S}{K_0} \quad (4)$$

$$T_{liquidus} = T_{melt} + m_S Y_S \quad (5)$$

Continuity Equation:

$$\frac{\partial(\rho Y_{s,liq})}{\partial t} + \nabla \cdot (\phi v Y_{s,liq}) = \nabla \cdot (\rho \phi v D_{s,m,liq} \nabla Y_{s,liq}) - K_0 Y_{s,liq} \frac{\partial[\rho(1-\phi)]}{\partial t} + \frac{\partial[\rho(1-\phi)] Y_{s,liq}}{\partial t} \quad (6)$$

Momentum Equation:

$$\frac{\partial(\rho v)}{\partial t} + \nabla \cdot (\rho v v) = -\nabla p + \mu \nabla^2 v + \rho g + \frac{(1-\phi)^2}{(\phi^2 + \varepsilon)} A_{mush} v \quad (7)$$

Energy Equation:

$$\frac{\partial(\rho H)}{\partial t} + \nabla \cdot (\rho v H) = \nabla \cdot (K \nabla T - \mathrm{h_s J_s}) \quad (8)$$

The formation of ice crystals is regulated by the methodology of solidification/melting. Within ANSYS Fluent, this phenomenon is depicted through an enthalpy–porosity approach called the "solidification/melting model", which manages a unified domain rather than a scenario involving multiphase flow. In this model, a liquid/solid mushy zone is integrated into the domain, acting as a permeable region. The porosity of this zone is determined by the proportion of liquid present, varying from 0 to 1 [101].

The liquid fraction can be ascertained using Equation (3), with T representing the local temperature, which defines the mushy zone's boundaries between the liquid and solid phases. The mushy zone is situated above the higher liquidus temperature ($T_{liquidus}$) and the lower solidus temperature ($T_{solidus}$) for a multicomponent mixture. These boundary temperatures can be calculated using Equations (4) and (5). In these equations, T_{melt} denotes the melting point of pristine water, whereas K_0 signifies the ratio of the solute's mass fraction in the solid phase to that in the liquid phase at the interface, which is proportionally related to the initial salinity. m_s is the slope of the liquidus line with respect to the local solute mass fraction, Y_S.

In the brine solution's solidification process, the S model delineates the repartitioning and stratification of salt between the solid and liquid phases, presupposing an absence of salt diffusion within the solidified region. In this model, a nonlinear correlation is established between the liquid fraction and the temperature at the interface, consequently, the altered continuity equation is depicted in Equation (6). In this equation, ρ denotes the density, $Y_{s,liq}$ represents the salt mass fraction in the liquid region, v is the liquid velocity, and $D_{s,m,liq}$ is the solute mass diffusion coefficient in the liquid phase.

The momentum equation is applied across the entire domain, with the resulting velocity field apportioned among various phases. To accommodate the pressure reduction due to the transition from water to ice, the fundamental momentum equation is modified by incorporating a suitable sink term [102]. The final momentum equation is presented in Equation (7), where p is the static pressure, μ is the molecular viscosity, g represents gravitational acceleration, A_{mush} is the mushy zone constant, and ε is a small value added to avoid division by zero. The energy equation in this model is shown in Equation (8), where H represents the overall enthalpy, k is the thermal conductivity, and $h_s J_s$ includes

species transport for solidification/melting problems. Specifically, h_s is the enthalpy of the salt species and J_s is the diffusion mass flux of salt.

Jayakody et al. [103] developed a 3D CFD model to simulate the freezing process of a single unit in salt solutions with salinity ranging from 1.5% to 4.5%, as illustrated in Figure 18. The model was validated against experimental data obtained from an instrumented ice maker. The results showed a maximum temperature deviation of 0.93%, a maximum ice salinity deviation of 15%, and a maximum brine salinity deviation of 13.1%.

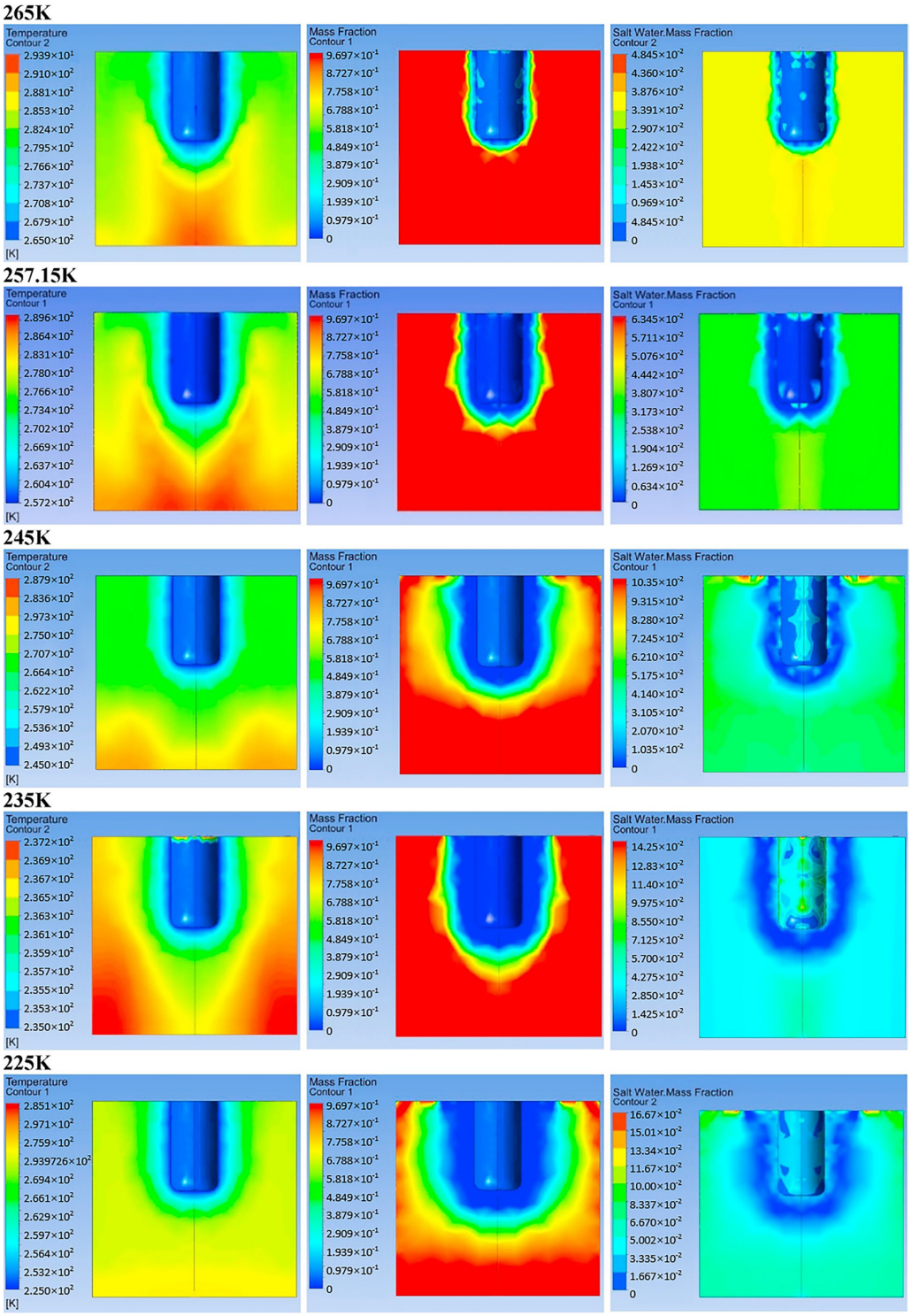

Figure 18. Temperature (**left**), liquid phase fraction (**middle**), and salt water mass fraction (**right**) contours for freezing temperatures of 265 K, 257.15 K, 245 K, 235 K, and 225 K [103].

EI Kadi et al. [104] performed a parametric analysis of indirect freeze desalination in a rectangular tray. They examined various factors, such as the salinity of the initial brine, the temperature of the ice source, and the temperature of the initial brine. The outcomes, illustrated in Figure 19, suggest that brine with a lower salt concentration tends to yield higher quality ice.

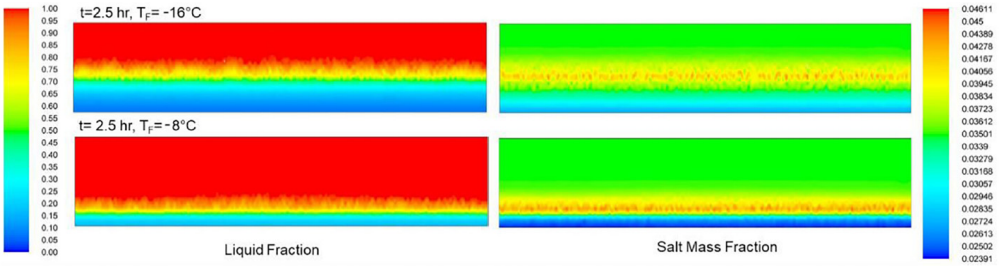

Figure 19. Contours of liquid fraction (**left**) and salt mass fraction (**right**) at a section of the FD system running under different freezing temperatures [104].

Savvopoulos et al. [105] conducted high-fidelity modeling of droplet freeze desalination for sustainable water purification and diverse applications. They compared and analyzed the brine cooling process under different conditions using CFD at both bulk and droplet scales. At a cooling temperature of −15 °C, Symeon conducted simulation using 5 µL saltwater droplets to analyze the temperature curve and solid-liquid mass fraction during the solid-liquid equilibrium stage under the influence of gravity. The results indicate that the influence of gravity on the local freezing dynamics of saline droplets becomes significant. As shown in Figure 20, the salt in the droplet begins to diffuse towards the liquid portion, mainly concentrated at the center and bottom of the droplet. Over time, this will result in the formation of a highly concentrated liquid area of 60 g/L at the bottom of the droplet, while ice with a salinity of 20 g/L accumulates at the top of the droplet. The study analyzed the concentration distribution and parameter changes along the vertical distance of droplets under different salt concentrations, and their effects on the freezing process and saltwater mass transfer inside the droplets, as shown in Figure 21. Researchers used CFD simulation to illustrate the concentration distribution of the salt content in droplets, demonstrating the intricate diffusion patterns of salt within droplets during ice formation.

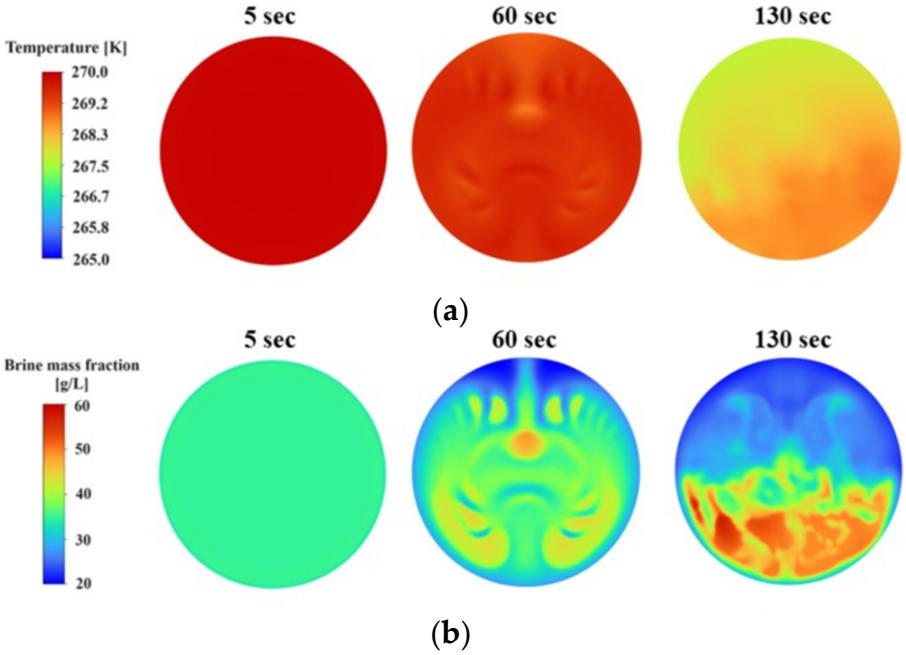

Figure 20. *Cont.*

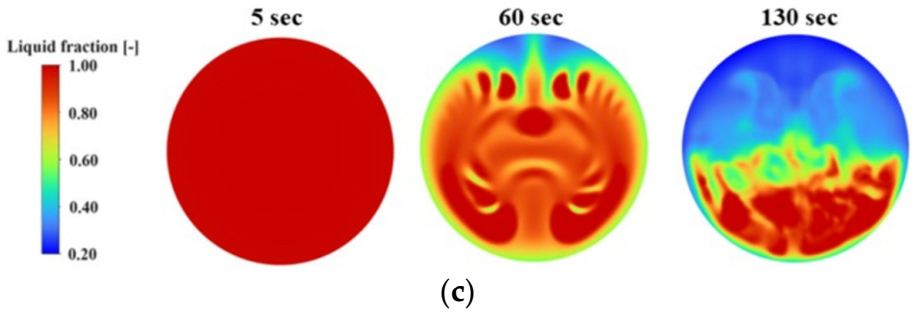

Figure 20. CFD simulation result of a 5 µL brine droplet during the equilibrium phase between liquid and ice at a cooling temperature of −15 °C: (**a**) temperature variation; (**b**) brine mass fraction changes; (**c**) liquid fraction alterations [105].

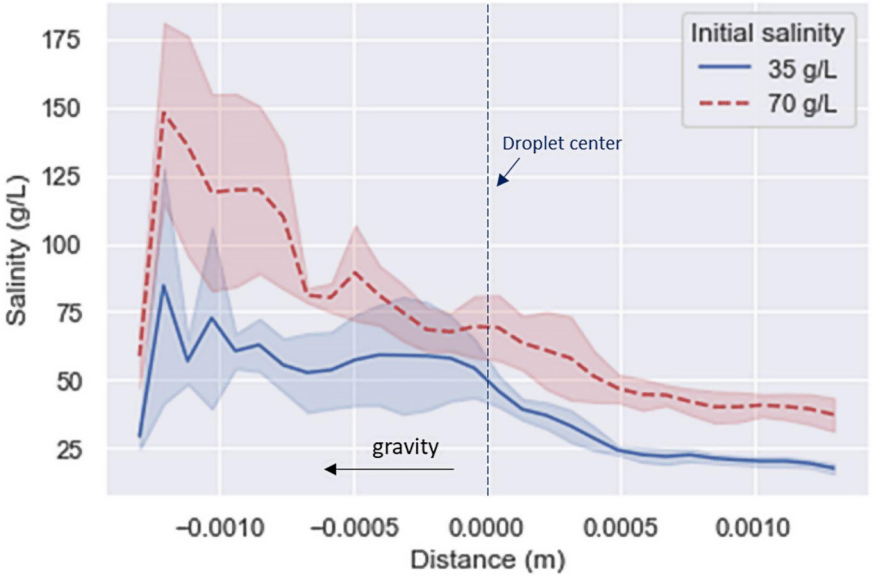

Figure 21. Concentration profile for 35 g/L vs. 70 g/L initially concentrated droplets along the vertical distance.

4.2. The Phase-Field Method

The phase-field method is widely used for mesoscopic-scale simulations, primarily to simulate the solidification process of two-dimensional and three-dimensional binary solutions. This method is based on the Ginzburg–Landau theory [106]. A continuously varying order parameter Φ is introduced to track the thermodynamic states of the two phases, thereby constructing the free energy form of each phase. The phase-field method is mainly used to model complex interfacial morphology changes and has been widely applied to processes such as solid-liquid phase transitions, two-phase flows, and solid-solid phase transitions during solidification. It effectively replicates the complex evolution of interfaces during solidification and has become an important tool for simulating mesoscopic structural evolution [107,108].

The phase-field method is centered on the Ginzburg–Landau theory, and based on statistical physics, it solves phase transition processes through differential equations while studying solute diffusion, ordering potentials, and thermodynamic driving forces.

The phase-field model couples the phase-field, temperature field, concentration field, and flow field, visualizing the crystallization process and directly displaying the formation of dendrites.

The following are the control equations of the phase-field method constructed based on the free energy density function.

Phase-field control equation:

$$\frac{\partial \varphi}{\partial t} = M[\varepsilon^2 \nabla^2 \varphi - \frac{\partial}{\partial x}(\varepsilon(\theta)\varepsilon'(\theta)\frac{\partial \varphi}{\partial y}) + \frac{\partial}{\partial y}(\varepsilon(\theta)\varepsilon'(\theta)\frac{\partial \varphi}{\partial x}) + \frac{RT}{V_m}h'(\varphi)In\frac{(1-c_L^e)(1-c_S)}{(1-c_S^e)(1-c_L)} - Wg'(\varphi)] \quad (9)$$

In the equation, t represents time, M represents the phase-field mobility, ε and W are phase-field parameters, $\varepsilon(\theta)$ is the anisotropy parameter, R is the gas constant, V_m is the molar volume, and C_S and C_L represent solute concentrations in the solid and liquid phases, respectively.

Concentration field control equation:

$$\frac{\partial c}{\partial t} = \nabla[D(\varphi)\nabla c] + \nabla[D(\varphi)h'(\varphi)(c_L - c_S)\nabla \varphi] \quad (10)$$

In the equation, $D(\phi)$ represents the solute diffusion rate, and D_S and D_L represent the solute diffusion coefficients in the solid and liquid phases, respectively.

Temperature field control equation:

$$\frac{\partial T}{\partial t} + \nabla \cdot (\overline{V}T) = D_T \nabla^2 T + \frac{1}{2}\frac{L}{C_p}\frac{\partial h(\varphi)}{\partial t} \quad (11)$$

In the equation, T represents temperature, L represents latent heat of crystallization, C_P represents specific heat, and D_T represents thermal diffusivity.

Yuan et al. [37] utilized the phase-field approach to model the development of ice crystal growth during the freeze desalination procedure of a binary water-NaCl mixture. Perturbation terms were introduced into the mathematical model to more accurately replicate the real crystallization process. As shown in Figure 22, when dendrites solidify, heat flow and disturbances influence their growth. The initial disturbance destabilizes the planar interface, causing it to transform into columnar dendrites. Competition among the dendrites causes some to grow more rapidly, which inhibits the growth of others. The faster-growing dendrites widen, further suppressing neighboring crystals and forming numerous small brine pockets. The tips of the dendrites grow quickly, and solute migrates toward their roots, but due to the slow diffusion rate, salt accumulates and raises the temperature at the root. This results in a decrease in supercooling and an increase in concentration that hinders growth at the root. In contrast, the central portion of the dendrite experiences less inhibition, leading to lateral growth. As the columnar crystals make contact, they form high-concentration brine cells, while growth at the upper part of the dendrite remains uninhibited.

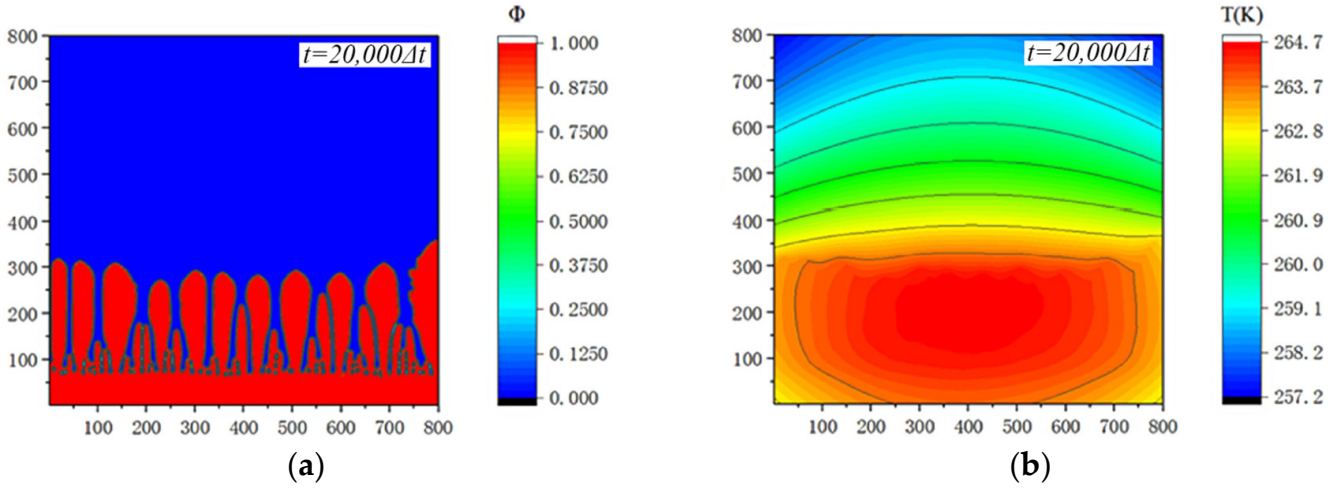

Figure 22. *Cont.*

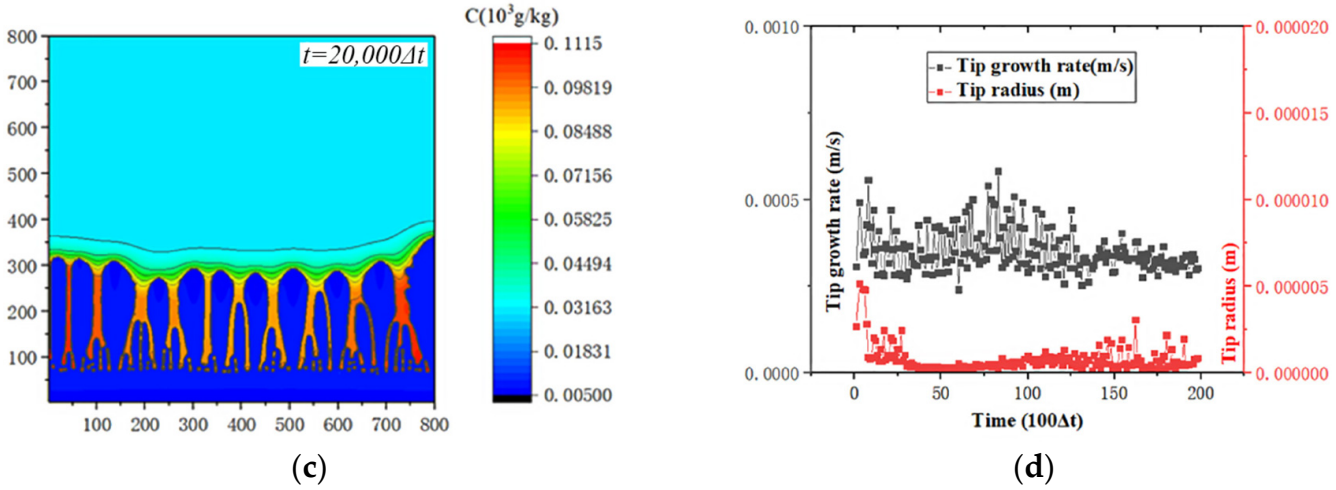

Figure 22. Results of directional crystallization of multiple crystal nuclei on horizontal wall: (**a**) phase-field results; (**b**) temperature field results; (**c**) concentration field results; (**d**) dendrite tip growth rate and tip radius [37].

Song et al. [91] proposed a novel coupled model combining the phase-field method (PFM) and the lattice Boltzmann method (LBM) for simulating sea ice crystallization, as illustrated in Figure 23. The study aimed to provide a comprehensive numerical approach to simulate sea ice crystallization, including phase change, solute migration, heat transfer, and fluid flow, while also exploring feasible control methods to enhance the efficiency of seawater freeze crystallization desalination. The study revealed that during the directional competitive growth of ice crystals, the salt content in ice decreased by 17.4% and 21.9% at growth rates of 0.025 m/s and 0.05 m/s, respectively. However, the ice crystal area also decreased by 21.8% and 25.3% at these same growth rates. Additionally, the presence of heterogeneous particles was found to narrow the brine channels, which in turn increased both the growth rate and the area of ice crystals

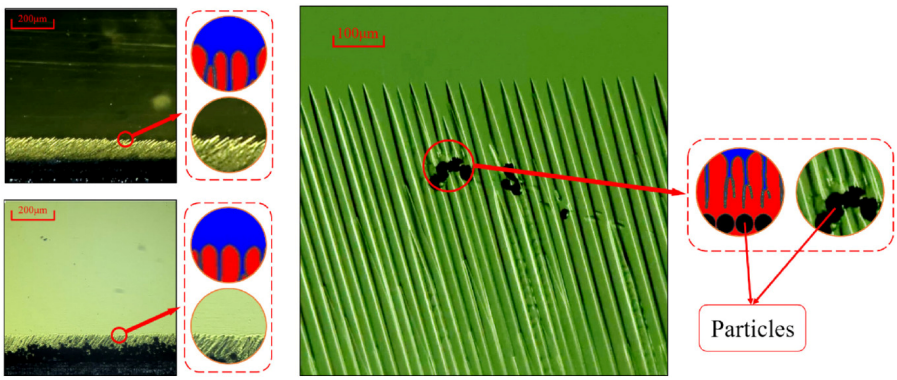

Figure 23. Comparison of experimental and simulation results of directional competitive growth of ice crystals [91].

Zhang et al. [109] studied the phase transition process of seawater crystallization in narrow channels using the phase-field method coupled with the lattice Boltzmann method, and investigated the efficiency of seawater desalination. As illustrated in Figure 24, at the initial stage, ice crystals grow directionally, leading to a continuous increase in the thickness of the ice layer at the bottom. As the process continued, the ice crystals differentiated into dendritic structures. Salts accumulate in the dendrite interstices, forming high-concentration brine pockets, which subsequently inhibit the growth of the bottom dendrites. The study indicates that the inlet temperature of the seawater and the heat flux have a significant impact on the efficiency of seawater desalination. As the inlet temperature

of the seawater increases, the salinity concentration in the ice crystals gradually decreases, while higher heat flux led to an increase in ice crystal salinity.

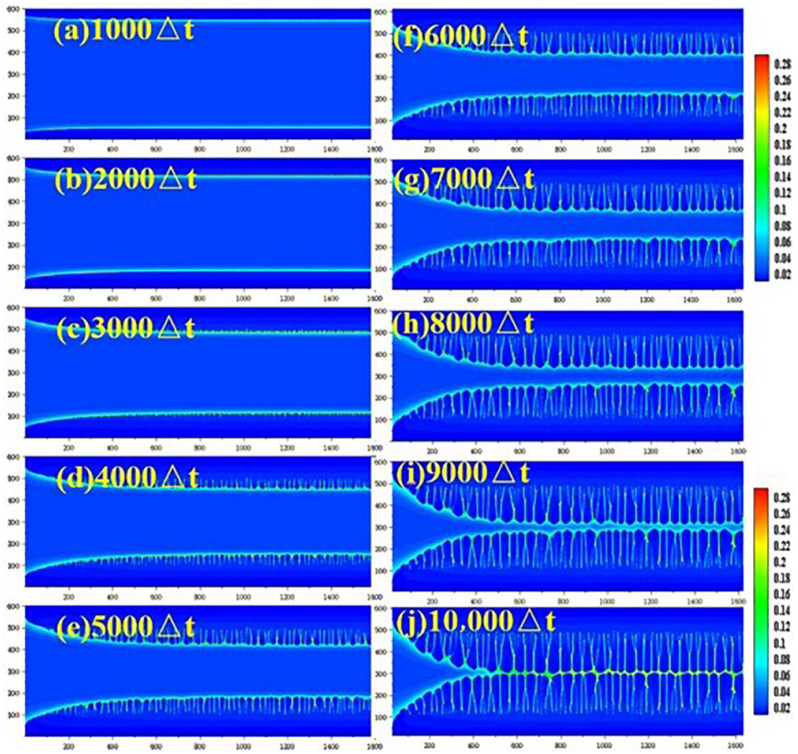

Figure 24. Concentration field of ice crystal growth in channels at different times:(**a**) 1000Δt; (**b**) 2000Δt; (**c**) 3000Δt; (**d**) 4000Δt; (**e**) 5000Δt; (**f**) 6000Δt; (**g**) 7000Δt; (**h**) 8000Δt; (**i**) 9000Δt; (**j**) 10,000Δt [109].

Song et al. [93] investigated how magnetic fields influence ice crystal growth and the formation and removal of brine pockets, using the phase-field and lattice Boltzmann methods. As shown in Figure 25, the study demonstrated that magnetic fields enhance the desalination rate of ice crystals. The application of a direct current (DC) magnetic field was found to significantly affect ice crystal growth, increasing the desalination rate and promoting the formation of brine pockets on the ice crystal surface. In comparison, the alternating current magnetic field had a smaller impact on ice crystals. Additionally, the use of a stepped magnetic field was effective in reducing the formation of brine pockets on the ice crystal surface.

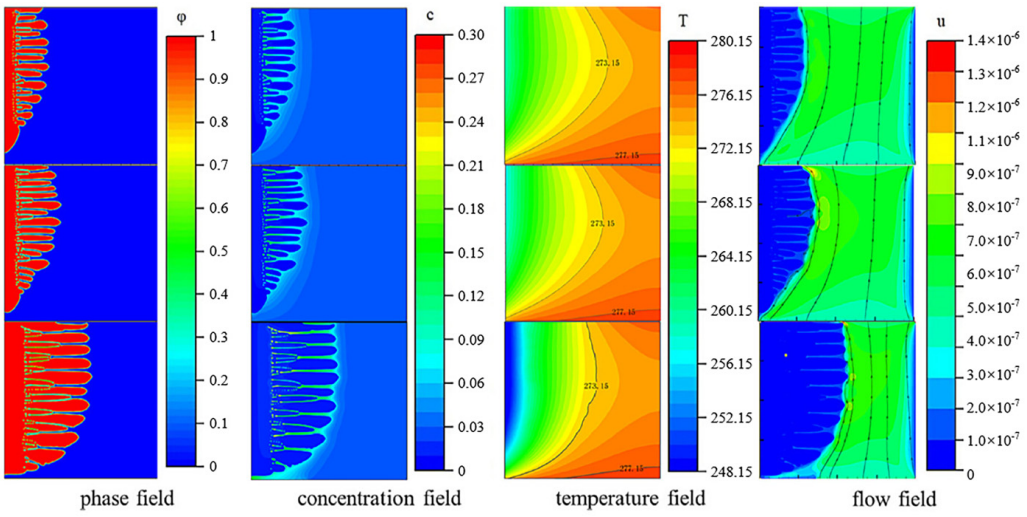

Figure 25. Distribution of each field under different magnetic field strengths [93].

4.3. Molecular Dynamics (MD)

The swift progress in molecular dynamics modeling has markedly enhanced research into the molecular-scale freezing phenomena in seawater desalination processes. MD simulations provide a method to analyze molecular mechanisms using numerical techniques and classical Newtonian equations. These simulations have been instrumental in studying various phenomena, including macromolecule behavior, protein folding, crystal nucleation, deformation processes, and nanoengineering [110].

The simulation equation can be expressed as the following:

$$\langle \overline{q} \rangle = \overline{q}^{B}_{ice} + \frac{\overline{q}^{B}_{ice} - \overline{q}^{B}_{water}}{2} [\tanh(\frac{x - x^{*}}{w}) + c] \quad (12)$$

where $\overline{q}^{B}_{ice}$ and $\overline{q}^{B}_{water}$ are the order parameters for bulk ice and water, w is the width of the interfacial region, c is a constant, and x^* represents the location of the interface.

The ion rejection rate is calculated as follows using Equation (13), based on the position of the ice-water interface:

$$R_R = (1 - \frac{C_I}{C_L}) \quad (13)$$

where C_I is the ratio of the number of ions trapped in the ice to the number of ice molecules and C_L is the initial salt concentration in the solution.

The radial distribution function describes the probability of finding a particle (such as a molecule or ion) at a specific distance from a reference particle. It is commonly used to analyze the interactions between two particles. The RDF can be computed as:

$$g(r) = \frac{V}{N_0^2} \sum_{i=1}^{N} \sum_{j \neq i}^{N} \delta(r - r_{ij}) \quad (14)$$

where V is volume, N_0 is the total number of water/ice molecules, δ is Dirae's delta function, and r_{ij} is distance between particles i and j.

Current research primarily focuses on water–NaCl systems [111], investigating aspects such as freezing point depression [112], salt solubility [113], surface tension [112], and the mechanisms and kinetics of ion rejection and inclusion in freeze desalination systems [114]. The freeze desalination systems are shown in Figure 26.

Luo et al. [115] employed molecular dynamics simulations to explore the microscopic mechanisms underlying ion rejection during the freezing of sodium chloride aqueous solutions. Their research uncovered that the hydration energy of ion-water interactions surpasses that of ion-ice interactions, which fundamentally drives the ion rejection process during freezing. The probability of ions being rejected by the ice is governed by the interplay between the energy barrier at the ice-water interface and thermal effects.

Tsironi et al. [116] combined X-ray diffraction with molecular dynamics simulations to study the freezing process of NaCl solutions across various brine concentrations, ranging from seawater conditions to saturation. The freezing process of NaCl solutions are shown in Figure 27. Their study demonstrated that ion inclusions, caused by the formation of $NaCl{\cdot}2H_2O$ hydrates are another source of salt in the ice. The simulations estimated that the concentration of ions trapped in the ice is around 0.5%. This value is significantly lower than the initial NaCl concentration of 3%, and it falls near the upper salinity limit for freshwater, with typical drinking water containing around 0.1% salinity and agricultural water up to 0.5%.

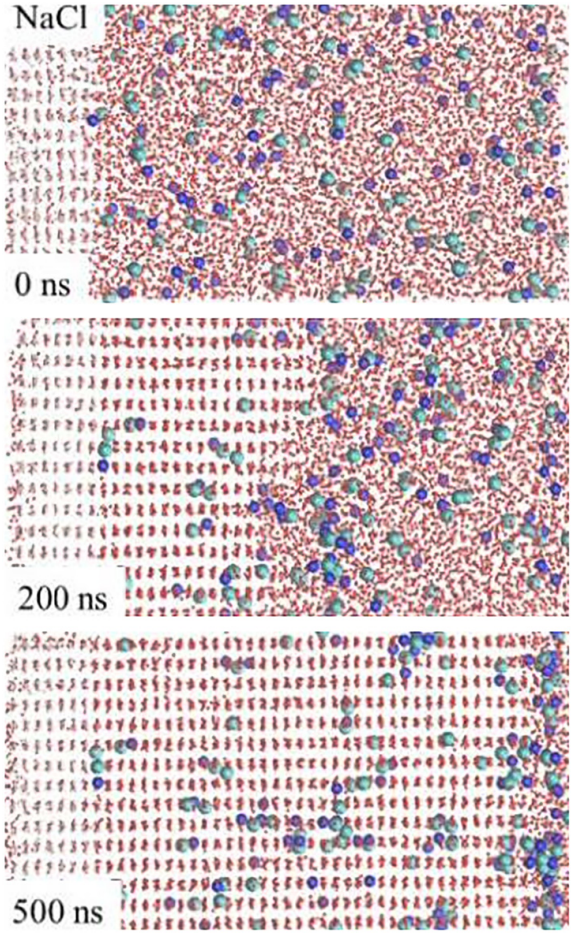

Figure 26. Snapshots of the molecular dynamics simulations for growth of ice in NaCl solutions at 245 K. Na^+, and Cl^- are represented by blue and cyan spheres, respectively. Only the oxygen atoms of water molecules are depicted by red spheres, shown in both the ice and solution [114].

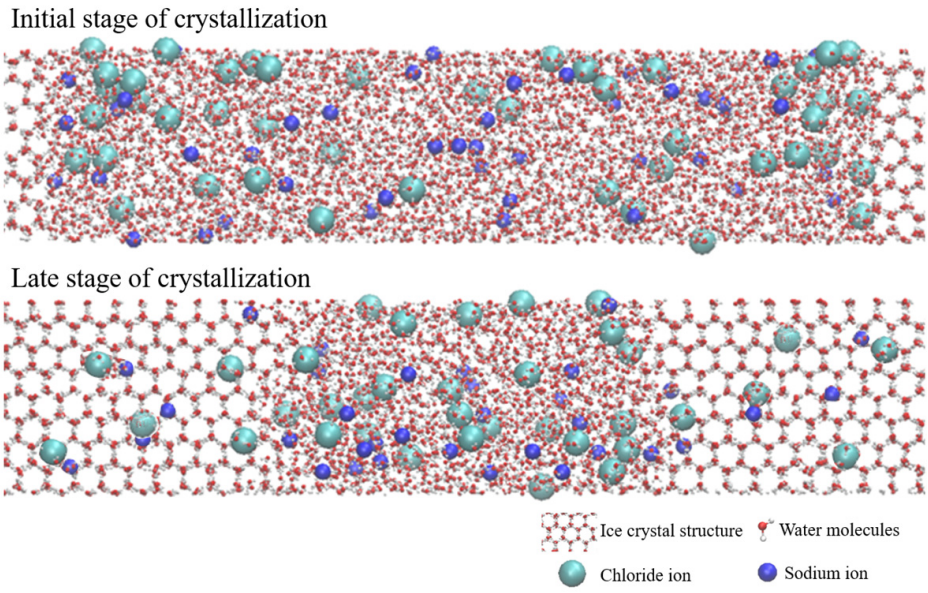

Figure 27. Molecular dynamics simulation of the microscopic mechanism underlying ion repulsion during the freezing of sodium chloride aqueous solution [116].

4.4. Summary

Simulation methods serve as an in-depth verification of experimental research, revealing the principles and underlying logic of seawater freezing desalination experiments, and are an important tool in advancing the development of freezing desalination technology. This section provides an overview and analysis of the three main simulation methods currently in use: CFD, the phase-field method, and molecular dynamics. In the field of seawater freezing desalination, CFD is the most widely used simulation method. By utilizing ANSYS Fluent software, parameters such as environmental temperature, boundary control, and heat and mass transfer processes are controlled, and ice crystal growth dynamics are introduced to simulate the ice crystal growth and salt separation processes. Many researchers have used CFD to simulate the crystallization of solutions with varying salt concentrations, ice crystal growth in different crystallizers, and the destruction and reconstruction of ice crystal structures. These studies have validated the accuracy of experiments in terms of desalination efficiency, crystal growth, and ice crystal purification on a macroscopic scale. The phase-field method, a mesoscale simulation technique for ice crystal growth, has unique advantages in handling solid-phase growth, liquid-phase flow, and solid-liquid interface changes. It can explore ice crystal growth under different conditions while analyzing the formation mechanism of salt cells. The phase-field method has evolved from simulating ice crystal growth to modeling it under different field properties, forming a correlation with experimental results. Experimental data can be used to update and refine the simulation program, ensuring the simultaneous development of experiments and simulations. Molecular dynamics simulations focus on molecular-level processes in seawater freezing desalination. They allow for tracking the dynamic changes of water molecules, sodium ions, chloride ions, and other elements during crystallization, while also studying the inclusion and exclusion phenomena of ions during phase transitions. Many researchers have used molecular dynamics simulations to study the behavior of ions within the ice crystal structure during crystallization, revealing the microscopic mechanisms behind ice crystal desalination. This has enabled a molecular-level understanding of the desalination process. Through these simulation methods, researchers can further optimize seawater freezing desalination technologies, thus advancing their development towards practical applications.

5. Current State of Development of Seawater Freezing Desalination

With the growing demand for fresh water, seawater freezing desalination technology began gain attention in the mid-20th century [117] as a potential method for desalinating seawater. Early research mainly focused on small-scale laboratory experiments to explore its feasibility [118]. Theoretically, seawater freezing desalination has certain advantages, but its development history is relatively short, and there are some notable drawbacks at the current stage. Compared to other desalination technologies, its application is relatively limited. This section discusses the advantages and challenges of the development of seawater freezing desalination technology and outlines potential directions for its future development.

5.1. Development Advantages

5.1.1. Resource Consumption

Seawater freezing desalination can utilize cost-effective alternative or waste energy sources, such as natural cold sources in high-latitude regions during winter [119], waste heat-driven thermoacoustic engine and refrigeration [120], or liquefied natural gas (LNG) cold energy [121]. This makes seawater freezing desalination more attractive in terms of energy consumption. For comparison, multi-stage flash distillation requires 4–6 kWh of energy to produce one ton of fresh water, while small-scale single-pass reverse osmosis units typically consume 6–10 kWh/m^3 of energy [122,123]. Antonelli et al. [75] proposed a method for seawater desalination using LNG. Each ton of LNG can produce 3.2 tons of desalted water. Under ideal conditions, a terminal with an annual processing capacity of 510.9 million cubic meters of natural gas could produce 10,000 tons of water per year,

which is equivalent to the needs of a town of 40,000 inhabitants. Mehdi Salakhi et al. [35] found that lowering the LNG inlet temperature from −10 °C to −60 °C increased the ice production from 60.9 g to 977.6 g. By increasing the Reynolds number of LNG from 4000 to 32,000, the ice production increased by 492 g, but the salinity of the ice also increased from 1.22% to 1.56%. For a Reynolds numbers below 16,000, potable water can be obtained after three stages of desalination. Chen et al. [89] studied seawater desalination through supercooled water dynamic ice making, finding that the electricity consumption for producing fresh water under these conditions is 6.7 kWh/m^3. Compared to the traditional seawater desalination methods used in large-scale commercial applications, freeze desalination offers significant advantages in terms of waste energy utilization and resource consumption.

5.1.2. Environmental Protection

The concentrated brine produced during industrial processes may lead to the degradation of local soil and ecosystems. Seawater freeze desalination technology does not impose stringent requirements on the salt concentration of the liquid, allowing it to process brine of various concentrations. This can reduce the environmental impact of wastewater from desalination processes or other industrial production. For brine near the eutectic concentration, freeze desalination is more effective in treating the concentrated brine [124]. Compared to MD, the three-stage process of FD can achieve approximately 2.3 times the salt recovery rate [14]. Eutectic freeze crystallization has also successfully been used for the treatment of RO brines, achieving 97% recoveries in the form of ice and salts [124]. In terms of carbon emissions, producing one cubic meter of freshwater via reverse osmosis (RO) generates 1.7–2.8 kg of CO_2, while multi-effect distillation (MED) emits 7–17.6 kg/m^3, and multi-stage flash distillation (MSF) emits 15.6–25 kg/m^3 [125]. At present, seawater freeze desalination has not yet been widely applied on a large scale. Its actual carbon emissions largely depend on the type of energy used and the efficiency of the technology. When LNG cold energy or solar energy are utilized, the carbon emissions can be nearly negligible.

5.1.3. Cost Advantage

Due to the current state of development of seawater freeze desalination, its present economic costs are based on data obtained from experimental studies. Wang et al. [31] developed a freeze desalination-membrane distillation (FD–MD) hybrid process utilizing liquefied natural gas (LNG) cold energy. This process produces ultrapure water with a salinity as low as 0.062 g/L, and achieves a total water recovery rate of up to 71.5% at a cost of 0.4 US$/$m^3$. Chen et al. [89] used seawater desalination through supercooled water dynamic ice making, reducing the production cost of freshwater to 0.6 US$/$m^3$. The production cost of freshwater using reverse osmosis (RO) ranges from 0.5 to 1.7 US$/$m^3$, the production costs using multi-effect distillation (MED) and multi-stage flash (MSF) range from 1.1 to 2.0 US$/$m^3$ and 1.9 to 2.5 US$/$m^3$, respectively [126,127]. In the future, with the large-scale application of seawater freeze desalination technology, the cost of freshwater production is expected to decrease, making it more economically valuable compared to traditional desalination methods.

5.2. Development Challenges

5.2.1. Freshwater Quality

Based on the principle of sea ice formation, theoretically, the freshwater produced by seawater freezing desalination has relatively high quality. However, due to the limitations of technological development, the current freshwater produced by seawater freezing desalination is difficult to directly use as drinking water or domestic water without further treatment. To improve the quality of freshwater production, researchers are currently focusing on pre-treatment and Post-treatment methods for the freezing process to reduce the salt concentration in the ice crystals. Song et al. [91] utilized seawater flow to alter the ice crystal growth process, finding that at a seawater flow rate of 0.025 m/s, the salt content in the ice crystals decreased by 17.4%. When the flow rate was 0.05 m/s, the salt content

in the ice crystals decreased by 21.9%. Additionally, Song simulated ice crystal growth under heterogeneous nucleation conditions, and the results indicated that the salt content in the ice crystals decreased by approximately 14.8%. D.G. Randal et al. [124] improved ice crystal quality by using the sweating technique. Songlee Han et al. [128] used centrifuging, washing, and sweating to treat ice crystals. Centrifuging achieved an average desalination efficiency of 96%. Washing with an appropriate amount of freshwater effectively increased the salt removal rate to 93%. Timely sweating also reduced the salt on the crystal surface by more than 95%.

Compared to freeze desalination, other desalination methods can drastically reduce salt levels. The optimized NBM presented 99.5% under SWRO testing conditions, with 50 bar applied pressure and a 32,000 mg/L NaCl feed solution concentration [129]. Porous hydrophobic PPO/PS membranes were prepared via the NIPS method, permeate flux over 28 kg/m^{2}h, and high salt rejection of 99.9% were obtained [127].

5.2.2. Crystallization Control

Due to the random occurrence of nucleation during seawater freezing desalination, it is impossible to control the start time of crystallization, the crystallization temperature, and the quality of the ice crystals. This significantly increases the technical difficulty of controlling the freezing crystallization process. Several scholars have conducted research on this issue using methods such as electric fields and microwaves to control nucleation. Marta Orlowska et al. [130] applied a static electric field ranging from 0 to 6.0 $\times$ 10^6 V/m in the crystallization vessel. Their results showed that as the applied voltage increased, the nucleation temperature shifted to higher values, demonstrating the capability of the static electric field to induce ice crystal nucleation at the desired supercooling degree. Similarly, Yang et al. [95] used microwaves to intervene in the crystallization process. Their experimental results found that the desalination efficiency significantly increased under the influence of microwaves. When the microwave treatment time was increased from 60 s to 240 s, the removal efficiencies of Cl^-, Mg^{2+}, Ca^{2+}, and total dissolved solids (TDS) increased from 74.33%, 81.41%, 51.16%, and 74.17% to 90.98%, 89.03%, 83.26%, and 91.05%, respectively. However, this also resulted in the ice production rate decreasing from 44.32% to 16.70%.

5.2.3. Investment Costs

Currently, laboratory freeze desalination experiments are primarily conducted on a small scale, and researchers have yet to accurately predict the costs associated with large-scale implementation [131]. Although there are various freeze desalination methods, the lack of large-scale applications results in relatively high initial investment costs and significant trial and error risks [132,133]. Moreover, the salt concentration of freshwater produced by different techniques is susceptible to external factors, potentially leading to product quality instability, which could affect market sales and regular business operations [134].

The greatest advantage of seawater desalination lies in achieving efficient freshwater production with minimal energy use. However, if existing cold sources such as LNG are utilized, a comprehensive environmental assessment and impact analysis are necessary, encompassing effects on marine ecology, noise, and emissions [135,136]. When using large compressors as a cold source, the coefficient of performance (COP) is the key factor determining costs. Currently, the energy consumption for laboratory-scale freeze desalination is approximately 7 kilowatts per ton of freshwater produced. Considering equipment investment, environmental factors, and operational costs, and given the current freshwater market price of about $1 to $3 per ton, the return on investment could potentially take 10 to 20 years, or even longer [137–139].

5.3. Integrated Development of Multiple Technologies

Due to the limitations of using a single seawater freezing desalination method in of optimal desalination effectiveness, many researchers have proposed a multi-technology integrated approach to seawater desalination. In this approach, freezing desalination is used as a pre-treatment method for other desalination technologies to reduce the energy consumption, freshwater yield, and freshwater quality issues associated with traditional desalination methods.

FD–MD [31] was demonstrated using indirect-contact freeze desalination (ICFD) and direct contact membrane distillation (DCMD) configurations. In the ICFD process, drinking water with a salinity of approximately 0.144 g/L was produced. Meanwhile, through the DCMD process, ultrapure water with a salinity of 0.062 g/L was obtained under high energy efficiency conditions. This process is an energy-efficient method, using LNG cold energy to reduce overall energy consumption. If only the heating power is considered, its specific energy consumption is 2.343 kWh/m^3. When both heating and cooling power are considered, this value increases to 4.633 kWh/m^3. This is roughly equivalent to the calculated specific energy consumption of RO, which is approximately 3.5 kWh/m^3.

Ibtissam Baayyad et al. [140] studied an industrial hybrid seawater desalination process by combining freezing system with reverse osmosis. In this system, the freezing process is used as a seawater pre-treatment method for RO. By combining freezing and membrane desalination, the hybrid system's performance was successfully improved. Compared to traditional RO desalination, the quality of the permeate water was improved by approximately 71%.The industrial hybrid seawater desalination process reduces the salinity of seawater from 35 g/L to approximately 0.111 g/L, while the water quality of traditional RO is about 0.387 g/L. Additionally, the total energy consumption of the process is estimated to be 5.171 kWh/m^3, which is lower than the 6.95 kWh/m^3 of traditional reverse osmosis processes, reducing energy consumption by 25%.

A. Zambrano et al. [141] proposed freeze desalination by the integration of falling film and block freeze-concentration techniques. The process produces water at a rate of 743.1 kg/h, with a solution containing 0.05% salt concentration accounting for 74% of the total, and a solution of 13.4% salt concentration making up the remaining 26%. This demonstrates the technical feasibility of the process. With a COP of 8, the electrical consumption is 59.2 kWh, which is equivalent to 11.5 kWh per 1000 kg of ice production. If an effluent of 603 kg/h at 3.7% can be returned to the water source, the energy consumption decreases to 23.1 kWh for the overall the process.

Kang Jia Lu et al. [142] developed a mathematical model for a zero liquid discharge desalination (ZLDD) system, which integrates freeze desalination (FD) and membrane distillation crystallization (MD-C), based on heat and mass transfer theories as well as experimental results. Seawater undergoes freeze desalination, producing fresh water and brine. The brine is treated by direct contact membrane distillation, resulting in fresh water and concentrated brine. The concentrated brine is then supplied to a cooling crystallizer, producing salt and ice crystals, thus achieving zero liquid discharge. Under laboratory conditions, the ZLDD system, with a seawater processing capacity of 72 kg/d, produces 2.52 kg of salt and 69.48 kg of water daily. The system's daily thermal and cooling energy consumption are 58.3 kWh and 59.8 kWh. It utilizes solar panels for electricity and LNG for daily cooling energy. The FD–MD–C system achieves a water recovery efficiency exceeding 74% in the production of potable water.

6. Conclusions

This paper systematically summarizes the development of seawater freezing desalination technologies. Compared to traditional methods such as thermal and membrane desalination, freezing desalination offers lower resource consumption, higher freshwater output, strong environmental adaptability, and notable economic advantages. However, its complexity, lower desalination rate, and high initial investment hinder widespread adoption. Despite these challenges, due to its enormous potential, freezing desalination is

becoming a research focus in the field of seawater desalination, with promising prospects for technological development and commercial applications.

Currently, seawater freeze desalination mainly employs the direct and indirect freezing desalination methods. The hydrate, eutectic, and vacuum freezing desalination methods are still limited to the research and verification stages due to technical constraints and high promotion costs.

Experimental research on seawater freeze desalination is currently focused on increasing freshwater production and improving desalination efficiency. Future trends in freeze desalination research are expected to include the optimization of freezing technologies, the application of new materials, and improvements in the structure of freezing devices.

The simulation of freeze crystallization has achieved full-scale coverage. From macroscopic CFD to mesoscopic phase-field methods, down to the microscopic realm of molecular dynamics, these approaches enable experimental comparisons and theoretical analyses of the entire freeze crystallization process from different perspectives, thereby advancing research into the freeze desalination process.

With the maturation of technology and the reduction of costs, seawater freezing desalination is expected to achieve large-scale commercial application, becoming an important freshwater supply method for coastal and water-scarce regions. As the technology advances, combining it with other desalination technologies, such as reverse osmosis and distillation, will enable the creation of hybrid desalination systems that optimize resource use while improving freshwater yield and quality. Additionally, the use of renewable energy sources such as solar and wind power to supply energy for the seawater freezing desalination system will reduce dependence on fossil fuels, making this a key direction for the sustainable development of freezing desalination technology.

Author Contributions: Conceptualization, S.Z. and H.Y.; methodology, S.Z.; software, S.Z.; formal analysis, R.Z.; investigation, R.Z.; resources, R.Z.; data curation, R.Z.; writing—original draft preparation, S.Z. and R.Z.; writing—review and editing, J.S.; visualization, S.Z. and J.S.; supervision, H.Y. and J.S.; project administration, H.Y.; funding acquisition, H.Y. All authors have read and agreed to the published version of the manuscript.

Funding: This research was funded by the National Natural Science Foundation of China, grant number 52476094, Shandong Provincial Natural Science Foundation, grant number ZR2023ME146, and the National Natural Science Foundation of China, grant number 52401352, Postgraduate Education Joint Cultivation Base Construction Projects, Ocean University of China, grant number HDYJ23005.

Institutional Review Board Statement: Not applicable.

Informed Consent Statement: Not applicable.

Data Availability Statement: The data that support the findings of this study are available in the ScienceDirect database at https://www.sciencedirect.com/, accessed on 18 September 2024. The queries used to retrieve the data are explained in this article.

Conflicts of Interest: The authors declare no conflicts of interest.

References

1. Sahu, P. A comprehensive review of saline effluent disposal and treatment: Conventional practices, emerging technologies, and future potential. *Water Reuse* **2021**, *11*, 33–65. [CrossRef]
2. World Population Prospects 2024: Summary of Results. Available online: https://desapublications.un.org/publications/world-population-prospects-2024-summary-results (accessed on 1 July 2024).
3. UN World Water Development Report 2024: Water for Prosperity and Peace. Available online: https://www.unwater.org/publications/un-world-water-development-report-2024 (accessed on 19 March 2024).
4. Al-Obaidi, M.; Alsarayreh, A.A.; Rashid, F.L.; Sowgath, M.T.; Alsadaie, S.; Ruiz-García, A.; Khayet, M.; Ghaffour, N.; Mujtaba, I.M. Hybrid membrane and thermal seawater desalination processes powered by fossil fuels: A comprehensive review, future challenges and prospects. *Desalination* **2024**, *583*, 117694. [CrossRef]
5. Aryanti, P.T.P.; Afred, M.Y.; Wardani, A.K.; Lugito, G.; Kadja, G.T.M.; Wenten, I.G.; Khoiruddin, K. Ultra low-pressure reverse osmosis (ULPRO) membrane for desalination: Current challenges and future directions. *Desalination* **2023**, *560*, 116650. [CrossRef]

6. Janajreh, I.; Zhang, H.; El Kadi, K.; Ghaffour, N. Freeze desalination: Current research development and future prospects. *Water Res.* **2023**, *229*, 119389. [CrossRef]
7. Kalista, B.; Shin, H.; Cho, J.; Jang, A. Current development and future prospect review of freeze desalination. *Desalination* **2018**, *447*, 167–181. [CrossRef]
8. Shatat, M.; Riffat, S.B. Water desalination technologies utilizing conventional and renewable energy sources. *Int. J. Low Carbon Technol.* **2014**, *9*, 1–19. [CrossRef]
9. Liu, T.; Mauter, M.S. Heat transfer innovations and their application in thermal desalination processes. *Joule* **2022**, *6*, 1199–1229. [CrossRef]
10. Lim, Y.J.; Goh, K.; Kurihara, M.; Wang, R. Seawater desalination by reverse osmosis: Current development and future challenges in membrane fabrication—A review. *J. Membr. Sci.* **2021**, *629*, 119292. [CrossRef]
11. Rich, A.; Mandri, Y.; Bendaoud, N.; Mangin, D.; Abderafi, S.; Bebon, C.; Semlali, N.; Klein, J.; Bounahmidi, T.; Bouhaouss, A.; et al. Freezing desalination of sea water in a static layer crystallizer. *Desalination Water Treat.* **2010**, *13*, 120–127. [CrossRef]
12. Ida Water Security Handbook Points to Robust Increase in Desalination and Water Reuse for 2019. Available online: https://wcponline.com/wp-content/uploads/2019/01/01-02_IDA.pdf (accessed on 28 September 2024).
13. Ihsanullah, I.; Atieh, M.A.; Sajid, M.; Nazal, M.K. Desalination and environment: A critical analysis of impacts, mitigation strategies, and greener desalination technologies. *Sci. Total Environ.* **2021**, *780*, 146585. [CrossRef]
14. Naidu, G.; Zhong, X.; Vigneswaran, S. Comparison of membrane distillation and freeze crystallizer as alternatives for reverse osmosis concentrate treatment. *Desalination* **2018**, *427*, 10–18. [CrossRef]
15. Kolliopoulos, G.; Xu, C.; Martin, J.T.; Devaere, N.; Papangelakis, V.G. Hybrid forward osmosis–freeze concentration: A promising future in the desalination of effluents in cold regions. *J. Water Process Eng.* **2022**, *47*, 102711. [CrossRef]
16. Cole, D.M.; Shapiro, L.H. Observations of brine drainage networks and microstructure of first-year sea ice. *Geophys* **1998**, *103*, 21739–21750. [CrossRef]
17. Subramani, A.; Jacangelo, J.G. Emerging desalination technologies for water treatment: A critical review. *Water Res.* **2015**, *75*, 164–187. [CrossRef] [PubMed]
18. Williams, P.M.; Ahmad, M.; Connolly, B.S.; Oatley-Radcliffe, D.L. Technology for freeze concentration in the desalination industry. *Desalination* **2015**, *356*, 314–327. [CrossRef]
19. Erlbeck, L.; Wössner, D.; Kunz, T.; Rädle, M.; Methner, F.J. Investigation of freeze crystallization and ice pressing in a semi-batch process for the development of a novel single-step desalination plant. *Desalination* **2018**, *448*, 76–86. [CrossRef]
20. Wiegandt, H.F.; Von Berg, R.L. Myths about freeze desalting. *Desalination* **1980**, *33*, 287–297. [CrossRef]
21. Miller, J.E. *Review of Water Resources and Desalination Technologies*; US Department of Energy: Washington, DC, USA, 2003. [CrossRef]
22. Rahman, M.S.; Ahmed, M.; Chen, X.D. Freezing-Melting Process and Desalination: I. Review of the State-of-the-Art. *Sep. Purif. Rev.* **2006**, *35*, 59–96. [CrossRef]
23. Vaessen, R.J.C.; Seckler, M.M.; Witkamp, G.J. Heat transfer in scraped eutectic crystallizers. *Int. J. Heat Mass Transf.* **2004**, *47*, 717–728. [CrossRef]
24. Barduhn, A.J.; Manudhane, A. Temperatures required for eutectic freezing of natural waters. *Desalination* **1979**, *28*, 233–241. [CrossRef]
25. Dickey, L.C. Evaporation of water from agitated freezing slurries at low pressure. *Desalination* **1996**, *104*, 155–163. [CrossRef]
26. Rice, W.; Chau, D.S.C. Freeze desalination using hydraulic refrigerant compressors. *Desalination* **1997**, *109*, 157–164. [CrossRef]
27. Gibson, W.; Emmermann, D.; Grossman, G.; Johnson, R.; Modica, A.; Pallone, A. Spray freezer and pressurized counterwasher for freeze desalination. *Desalination* **1974**, *14*, 249–262. [CrossRef]
28. Barduhn, A.J. The state of the crystallization processes for desalting saline waters. *Desalination* **1968**, *5*, 173–184. [CrossRef]
29. Hirakawa, S.; Kosugi, K. Utilization of LNG cold. *Int. J. Refrig.* **1981**, *4*, 17–21. [CrossRef]
30. Gilliland, E.R. I&EC Lectures Fresh Water for the Future. *Ind. Eng. Chem.* **1955**, *47*, 2410–2422.
31. Wang, P.; Chung, T. A conceptual demonstration of freeze desalination-membrane distillation (FD–MD) hybrid desalination process utilizing liquefied natural gas (LNG) cold energy. *Water Res.* **2012**, *46*, 4037–4052. [CrossRef]
32. Xie, C.; Zhang, L.; Liu, Y.; Lv, Q.; Ruan, G.; Hosseini, S.S. A direct contact type ice generator for seawater freezing desalination using LNG cold energy. *Desalination* **2018**, *435*, 293–300. [CrossRef]
33. Liu, Y.; Ming, T.; Wu, Y.; de Richter, R.; Fang, Y.; Zhou, N. Desalination of seawater by spray freezing in a natural draft tower. *Desalination* **2020**, *496*, 114700. [CrossRef]
34. Jiang, Y.; Cao, C.; Fei, X.; Zhao, H.; Jin, L. Solute selectivity, separation mechanism and application performance of freezing wastewater treatment: Focus on air cooling and direct contact cooling. *J. Water Process Eng.* **2021**, *44*, 102445. [CrossRef]
35. Salakhi, M.; Eghtesad, A.; Afshin, H. Heat and mass transfer analysis and optimization of freeze desalination utilizing cold energy of LNG leaving a power generation cycle. *Desalination* **2022**, *527*, 115595. [CrossRef]
36. Kadi, K.E.; Janajreh, I. Desalination by Freeze Crystallization: An Overview. *Int. J. Therm. Environ. Eng.* **2019**, *15*. [CrossRef]
37. Yuan, H.; Sun, K.; Wang, K.; Zhang, J.; Zhang, Z.; Zhang, L.; Li, S.; Li, Y. Ice crystal growth in the freezing desalination process of binary water-NaCl system. *Desalination* **2020**, *496*, 114737. [CrossRef]
38. Miyawaki, O.; Liu, L.; Shirai, Y.; Sakashita, S.; Kagitani, K. Tubular ice system for scale-up of progressive freeze-concentration. *J. Food Eng.* **2005**, *69*, 107–113. [CrossRef]

39. Yuan, H.; Sun, P.; Zhang, J.; Sun, K.; Mei, N.; Zhou, P. Theoretical and experimental investigation of an absorption refrigeration and pre-desalination system for marine engine exhaust gas heat recovery. *Appl. Therm. Eng.* **2019**, *150*, 224–236. [CrossRef]
40. Najim, A. Modelling of heat transfer for progressive freeze desalination utilizing the vertical freezing apparatus. *Int. J. Therm. Sci.* **2023**, *192*, 108427. [CrossRef]
41. Mahdavi, M.; Mahvi, A.H.; Nasseri, S.; Yunesian, M. Application of Freezing to the Desalination of Saline Water. *Arab. J. Sci. Eng.* **2011**, *36*, 1171–1177. [CrossRef]
42. Medjani, K. Department of Engineering Xavier University of Louisiana New Orleans, LA 70125. *Int. Commun. Heat Mass Transf.* **1996**, *23*, 917–928. [CrossRef]
43. Chang, J.; Zuo, J.; Lu, K.; Chung, T. Freeze desalination of seawater using LNG cold energy. *Water Res.* **2016**, *102*, 282–293. [CrossRef] [PubMed]
44. Gao, W.; Smith, D.W.; Sego, D.C. Treatment of pulp mill and oil sands industrial wastewaters by the partial spray freezing process. *Water Res.* **2004**, *38*, 579–584. [CrossRef]
45. Hung, W.T.; Feng, W.H.; Tsai, I.H.; Lee, D.J.; Hong, S.G. Uni-directional freezing of waste activated sludges: Vertical freezing versus radial freezing. *Water Res.* **1997**, *31*, 2219–2228. [CrossRef]
46. Gay, G.; Lorain, O.; Azouni, A.; Aurelle, Y. Wastewater treatment by radial freezing with stirring effects. *Water Res.* **2003**, *37*, 2520–2524. [CrossRef]
47. Shin, H.; Kalista, B.; Jeong, S.; Jang, A. Optimization of simplified freeze desalination with surface scraped freeze crystallizer for producing irrigation water without seeding. *Desalination* **2019**, *452*, 68–74. [CrossRef]
48. Htira, T.; Cogné, C.; Gagnière, E.; Mangin, D. Experimental study of industrial wastewater treatment by freezing. *J. Water Process Eng.* **2018**, *23*, 292–298. [CrossRef]
49. Kaviani, R.; Shabgard, H.; Elhefny, A.; Cai, J.; Parthasarathy, R. Experimental and theoretical study of a novel freeze desalination system with an intermediate cooling liquid. *Desalination* **2024**, *576*, 117381. [CrossRef]
50. Curto, D.; Franzitta, V.; Guercio, A. A Review of the Water Desalination Technologies. *Appl. Sci.* **2021**, *11*, 670. [CrossRef]
51. Smith, P.; Martino, D.; Cai, Z.; Gwary, D.; Janzen, H.; Kumar, P.; McCarl, B.; Ogle, S.; O'Mara, F.; Rice, C.; et al. Greenhouse gas mitigation in agriculture. *Philos. Trans. R. Soc. B Biol. Sci.* **2008**, *363*, 789–813. [CrossRef]
52. Jeffry, L.; Ong, M.Y.; Nomanbhay, S.; Mofijur, M.; Mubashir, M.; Show, P.L. Greenhouse gases utilization: A review. *Fuel* **2021**, *301*, 121017. [CrossRef]
53. Zhang, J.; Chen, S.; Mao, N.; He, T. Progress and prospect of hydrate-based desalination technology. *Front. Energy* **2022**, *16*, 445–459. [CrossRef]
54. Liu, X.; Li, Y.; Chen, G.; Chen, D.; Sun, B.; Yin, Z. Coupling Amino Acid with THF for the Synergistic Promotion of CO_2 Hydrate Micro Kinetics: Implication for Hydrate-Based CO_2 Sequestration. *ACS Sustain. Chem. Eng.* **2023**, *11*, 6057–6069. [CrossRef]
55. Gautam, R.; Kumar, S.; Sahai, M.; Kumar, A. Solid CO_2 hydrates for sustainable environment: Application in carbon capture and desalination. *Mater. Today Proc.* **2022**, *67*, 609–615. [CrossRef]
56. Mavukkandy, M.O.; Chabib, C.M.; Mustafa, I.; Al Ghaferi, A.; AlMarzooqi, F. Brine management in desalination industry: From waste to resources generation. *Desalination* **2019**, *472*, 114187. [CrossRef]
57. Sahu, P. Clathrate hydrate technology for water reclamation: Present status and future prospects. *J. Water Process Eng.* **2021**, *41*, 102058. [CrossRef]
58. Pahlavanzadeh, H.; Javidani, A.M.; Ganji, H.; Mohammadi, A. Investigation of the Effect of NaCl on the Kinetics of R410a Hydrate Formation in the Presence and Absence of Cyclopentane with Potential Application in Hydrate-Based Desalination. *Ind. Eng. Chem. Res.* **2020**, *59*, 14115–14125. [CrossRef]
59. Zhang, X.; He, J.; Shan, T.; Liu, Q.; Yuan, Q.; Li, J.; Wu, Q.; Zhang, P. A comprehensive review on the characteristics and kinetics of freshwater separation by hydrate-based method: Current progress, challenges and perspectives. *Desalination* **2024**, *575*, 117279. [CrossRef]
60. Truong-Lam, H.S.; Seo, S.D.; Jeon, C.; Lee, G.; Lee, J.D. A gas hydrate process for high-salinity water and wastewater purification. *Desalination* **2022**, *529*, 115651. [CrossRef]
61. Babu, P.; Nambiar, A.; Chong, Z.R.; Daraboina, N.; Albeirutty, M.; Bamaga, O.A.; Linga, P. Hydrate-based desalination (HyDesal) process employing a novel prototype design. *Chem. Eng. Sci.* **2020**, *218*, 115563. [CrossRef]
62. Park, K.; Hong, S.Y.; Lee, J.W.; Kang, K.C.; Lee, Y.C.; Ha, M.; Lee, J.D. A new apparatus for seawater desalination by gas hydrate process and removal characteristics of dissolved minerals (Na^+, Mg^{2+}, Ca^{2+}, K^+, B^{3+}). *Desalination* **2011**, *274*, 91–96. [CrossRef]
63. Han, S.; Rhee, Y.; Kang, S. Investigation of salt removal using cyclopentane hydrate formation and washing treatment for seawater desalination. *Desalination* **2017**, *404*, 132–137. [CrossRef]
64. Ting, W.H.T.; Tan, I.A.W.; Salleh, S.F.; Abdul Wahab, N.; Atan, M.F.; Abdul Raman, A.A.; Kong, S.L.; Lam, L.S. Sustainable saline wastewater treatment using eutectic freeze crystallization: Recent advances, challenges and future prospects. *J. Environ. Chem. Eng.* **2024**, *12*, 112919. [CrossRef]
65. Randall, D.G.; Nathoo, J.; Lewis, A.E. A case study for treating a reverse osmosis brine using Eutectic Freeze Crystallization—Approaching a zero waste process. *Desalination* **2011**, *266*, 256–262. [CrossRef]
66. Van Spronsen, J.; Pascual, M.R.; Genceli, F.E.; Trambitas, D.O.; Evers, H.; Witkamp, G.J. Eutectic freeze crystallization from the ternary Na_2CO_3–$NaHCO_3$–H_2O system. *Chem. Eng. Res. Des.* **2010**, *88*, 1259–1263. [CrossRef]

67. Aspeling, B.J.; Chivavava, J.; Lewis, A.E. Selective salt crystallization from a seeded ternary eutectic system in Eutectic Freeze crystallization. *Sep. Purif. Technol.* **2020**, *248*, 117019. [CrossRef]
68. Hubbe, M.A.; Becheleni, E.M.A.; Lewis, A.E.; Peters, E.M.; Gan, W.; Nong, G.; Mandal, S.; Shi, S.Q. Recovery of Inorganic Compounds from Spent Alkaline Pulping Liquor by Eutectic Freeze Crystallization and Supporting Unit Operations: A Review. *Bioresources* **2018**, *13*, 9180. [CrossRef]
69. Lewis, A.E.; Nathoo, J.; Thomsen, K.; Kramer, H.J.; Witkamp, G.J.; Reddy, S.T.; Randall, D.G. Design of a Eutectic Freeze Crystallization process for multicomponent waste water stream. *Chem. Eng. Res. Des.* **2010**, *88*, 1290–1296. [CrossRef]
70. Mazli, W.N.A.; Samsuri, S.; Amran, N.A. Study of progressive freeze concentration and eutectic freeze crystallization technique for salt recovery. *IOP Conf. Series Mater. Sci. Eng.* **2020**, *778*, 12167. [CrossRef]
71. Leyland, D.; Chivavava, J.; Lewis, A.E. Investigations into ice scaling during eutectic freeze crystallization of brine streams at low scraper speeds and high supersaturation. *Sep. Purif. Technol.* **2019**, *220*, 33–41. [CrossRef]
72. Hasan, M.; Filimonov, R.; Chivavava, J.; Sorvari, J.; Louhi-Kultanen, M.; Lewis, A.E. Ice growth on the cooling surface in a jacketed and stirred eutectic freeze crystallizer of aqueous Na_2SO_4 solutions. *Sep. Purif. Technol.* **2017**, *175*, 512–526. [CrossRef]
73. Wang, J.; Cao, F. *Thermally-Driven Ejector for Vacuum Freezing Desalination at the Triple Point*; ASTFE Digital Library; Begel House Inc.: Redding, CT, USA, 2020. [CrossRef]
74. Najim, A. A review of advances in freeze desalination and future prospects. *Npj Clean Water* **2022**, *5*, 15. [CrossRef]
75. Attilio, A. Consultant Desalinated water production at LNG-terminals. *Desalination* **1983**, *45*, 383–390. [CrossRef]
76. Cao, W.; Lu, X.; Lin, W.; Gu, A. Parameter comparison of two small-scale natural gas liquefaction processes in skid-mounted packages. *Appl. Therm. Eng.* **2006**, *26*, 898–904. [CrossRef]
77. Lin, W.; Huang, M.; Gu, A. A seawater freeze desalination prototype system utilizing LNG cold energy. *Int. J. Hydrogen Energy* **2017**, *42*, 18691–18698. [CrossRef]
78. Seo, S.D.; Hong, S.Y.; Sum, A.K.; Lee, K.; Lee, J.D.; Lee, B.R. Thermodynamic and kinetic analysis of gas hydrates for desalination of saturated salinity water. *Chem. Eng. J.* **2019**, *370*, 980–987. [CrossRef]
79. Lee, S.H.; Park, K. Conceptual design and economic analysis of a novel cogeneration desalination process using LNG based on clathrate hydrate. *Desalination* **2021**, *498*, 114703. [CrossRef]
80. Amran, N.A.; Samsuri, S.; Safiei, N.Z.; Zakaria, Z.Y.; Jusoh, M. Review: Parametric Study on the Performance of Progressive Cryoconcentration System. *Chem. Eng. Commun.* **2016**, *203*, 957–975. [CrossRef]
81. Fujioka, R.; Wang, L.P.; Dodbiba, G.; Fujita, T. Application of progressive freeze-concentration for desalination. *Desalination* **2013**, *319*, 33–37. [CrossRef]
82. Eghtesad, A.; Salakhi, M.; Afshin, H.; Hannani, S.K. Numerical investigation and optimization of indirect freeze desalination. *Desalination* **2020**, *481*, 114378. [CrossRef]
83. Salajeghe, M.; Ameri, M. Thermodynamic analysis of single and multi-effect freeze desalination. *Appl. Therm. Eng.* **2023**, *225*, 120148. [CrossRef]
84. Mtombeni, T.; Maree, J.P.; Zvinowanda, C.M.; Asante, J.K.O.; Oosthuizen, F.S.; Louw, W.J. Evaluation of the performance of a new freeze desalination technology. *Int. J. Environ. Sci. Technol.* **2013**, *10*, 545–550. [CrossRef]
85. Jayakody, H.; Al-Dadah, R.; Mahmoud, S. Cryogenic Energy for Indirect Freeze Desalination—Numerical and Experimental Investigation. *Processes* **2020**, *8*, 19. [CrossRef]
86. Badawy, S.M. Laboratory freezing desalination of seawater. *Desalination Water Treat.* **2015**, *57*, 11040–11047. [CrossRef]
87. Zhang, H.; Janajreh, I.; Hassan Ali, M.I.; Askar, K. Freezing desalination: Heat and mass validated modeling and experimental parametric analyses. *Case Stud. Therm. Eng.* **2021**, *26*, 101189. [CrossRef]
88. Yang, H.; Sun, Z.; Zhan, Z.; Zhang, H.; Yao, Y. Effects of watering parameters in a combined seawater desalination process. *Desalination* **2018**, *425*, 77–85. [CrossRef]
89. Chen, D.; Zhang, C.; Rong, H.; Wei, C.; Gou, S. Experimental study on seawater desalination through supercooled water dynamic ice making. *Desalination* **2020**, *476*, 114233. [CrossRef]
90. Baayyad, I.; Hassani, N.S.A. Ice suspension crystallization pretreatment for a new hybrid seawater desalination process: Modeling, simulation, and parametric sensitivity study. *Desalination Water Treat.* **2017**, *95*, 34–44. [CrossRef]
91. Song, J.; Zhang, D.; Yuan, H.; Zhang, J.; Zhou, P.; Li, Y.; Wang, K.; Mei, N. Sea water frozen crystalisation impacted by flow and heterogeneous nucleation: PFM-LBM coupled modeling, simulation and experiments. *Desalination* **2022**, *524*, 115484. [CrossRef]
92. Wang, K.; Zhang, D.; Mei, N.; Zhang, J.; Li, Y.; Si, H.; Yuan, H. Inhibition effect of adsorption on brine pockets formation during seawater freeze desalination. *Desalination* **2022**, *526*, 115507. [CrossRef]
93. Song, R.; Wang, K.; Gong, M.; Yuan, H. Multi-physical field simulations of directional seawater freeze-crystallisation under a magnetic field. *Desalination* **2023**, *560*, 116687. [CrossRef]
94. Zhang, Y.; Wang, X.; Zhao, T.; Wang, X.; Liu, Y.; Zhao, C. Promotional effects of ultrasound and oscillation on sea ice desalination. *Sep. Purif. Technol.* **2024**, *347*, 127622. [CrossRef]
95. Yang, H.; Fu, M.; Zhan, Z.; Wang, R.; Jiang, Y. Study on combined freezing-based desalination processes with microwave treatment. *Desalination* **2020**, *475*, 114201. [CrossRef]
96. Liu, X.; Lan, W.; Ye, K.; Han, W.; Zhang, J.; Mohtaram, S.; Chen, L. Numerical simulation and experimental analysis of ice crystal growth and freezing-centrifugal desalination for seawater with different compositions. *Sep. Purif. Technol.* **2022**, *298*, 121656. [CrossRef]

97. Qin, F.G.F.; Chen, X.D.; Farid, M.M. Growth kinetics of ice films spreading on a subcooled solid surface. *Sep. Purif. Technol.* **2004**, *39*, 109–121. [CrossRef]
98. Qin, F.G.F.; Chen, X.D.; Free, K. Freezing on subcooled surfaces, phenomena, modeling and applications. *Int. J. Heat Mass Transf.* **2009**, *52*, 1245–1253. [CrossRef]
99. Qin, F.G.F.; Zhao, J.C.; Russell, A.B.; Chen, X.D.; Chen, J.J.; Robertson, L. Simulation and experiment of the unsteady heat transport in the onset time of nucleation and crystallization of ice from the subcooled solution. *Int. J. Heat Mass Transf.* **2003**, *46*, 3221–3231. [CrossRef]
100. Chivavava, J.; Rodriguez-Pascual, M.; Lewis, A.E. Effect of Operating Conditions on Ice Characteristics in Continuous Eutectic Freeze Crystallization. *Chem. Eng. Technol.* **2014**, *37*, 1314–1320. [CrossRef]
101. Zimmermann, N.E.R.; Vorselaars, B.; Quigley, D.; Peters, B. Nucleation of NaCl from Aqueous Solution: Critical Sizes, Ion-Attachment Kinetics, and Rates. *J. Am. Chem. Soc.* **2015**, *137*, 13352–13361. [CrossRef] [PubMed]
102. Voller, V.R.; Swaminathan, C.R. General source-based method for solidification phase change. *Numer. Heat Transf. Part B Fundam.* **1991**, *19*, 175–189. [CrossRef]
103. Jayakody, H.; Al-Dadah, R.; Mahmoud, S. Numerical investigation of indirect freeze desalination using an ice maker machine. *Energy Convers. Manag.* **2018**, *168*, 407–420. [CrossRef]
104. Kadi, K.E.; Janajreh, I. High-Fidelity Simulation and Parametric Analysis of Static Indirect Freeze Desalination Process. In Proceedings of the 2018 6th International Renewable and Sustainable Energy Conference (IRSEC), Rabat, Morocco, 5–8 December 2018; pp. 1–6. [CrossRef]
105. Savvopoulos, S.; El Kadi, K.; Zhang, H.; Janajreh, I. Droplet freeze desalination high fidelity modeling for sustainable water purification and diverse applications. *Desalination* **2024**, *586*, 117858. [CrossRef]
106. Rajantie, A. Vortices and the Ginzburg–Landau phase transition. *Phys. B Condens. Matter* **1998**, *255*, 108–115. [CrossRef]
107. Hohenberg, P.C.; Krekhov, A.P. An introduction to the Ginzburg–Landau theory of phase transitions and nonequilibrium patterns. *Phys. Rep.* **2015**, *572*, 1–42. [CrossRef]
108. Pan, H.; Han, Z.; Liu, B. Study on Dendritic Growth in Pressurized Solidification of Mg–Al Alloy Using Phase Field Simulation. *J. Mater. Sci. Technol.* **2016**, *32*, 68–75. [CrossRef]
109. Zhang, J.; Yuan, J.; Yuan, H. Numerical and experimental investigation of phase change characteristics and desalination effect of seawater freezing desalination in narrow channels. *Desalination* **2022**, *544*, 116145. [CrossRef]
110. Rasmussen, A.; Jannat, M.; Wang, H. Fundamentals of freeze desalination: Critical review of ion inclusion and rejection studies from molecular dynamics perspective. *Desalination* **2024**, *573*, 117216. [CrossRef]
111. Bianco, V.; Conde, M.M.; Lamas, C.P.; Noya, E.G.; Sanz, E. Phase diagram of the NaCl-water system from computer simulations. *J. Chem. Phys.* **2022**, *156*, 064505. [CrossRef] [PubMed]
112. Conde, M.M.; Rovere, M.; Gallo, P. Molecular dynamics simulations of freezing-point depression of TIP4P/2005 water in solution with NaCl. *J. Mol. Liq.* **2018**, *261*, 513–519. [CrossRef]
113. Benavides, A.L.; Aragones, J.L.; Vega, C. Consensus on the solubility of NaCl in water from computer simulations using the chemical potential route. *J. Chem. Phys.* **2016**, *144*, 124504. [CrossRef] [PubMed]
114. Zhang, S.; Zhang, C.; Wu, S.; Zhou, X.; He, Z.; Wang, J. Ion-Specific Effects on the Growth of Single Ice Crystals. *J. Phys. Chem. Lett.* **2021**, *12*, 8726–8731. [CrossRef]
115. Luo, S.; Jin, Y.; Tao, R.; Li, H.; Li, C.; Wang, J.; Li, Z. Molecular understanding of ion rejection in the freezing of aqueous solutions. *Phys. Chem. Chem. Phys.* **2021**, *23*, 13292–13299. [CrossRef]
116. Tsironi, I.; Schlesinger, D.; Späh, A.; Eriksson, L.; Segad, M.; Perakis, F. Brine rejection and hydrate formation upon freezing of NaCl aqueous solutions. *Phys. Chem. Chem. Phys.* **2020**, *22*, 7625–7632. [CrossRef]
117. Walter, W. Rinne, Desalting Sea Water by Refrigeration Processes: Désalinisation de l'eau de mer par le froid. *Prog. Refrig. Sci. Technol.* **1965**, 1469–1473.
118. Landau, M.; Martindale, A. Assessment of crystalliser designs for a butane freeze desalination process. *Desalination* **1967**, *3*, 318–329. [CrossRef]
119. Hasan, M.; Louhi-Kultanen, M. Water purification of aqueous nickel sulfate solutions by air cooled natural freezing. *Chem. Eng. J.* **2016**, *294*, 176–184. [CrossRef]
120. Fazli, M.; Mazaheri, K. Energy, Exergy, and flow fields analysis to enhance performance potential of a heat-driven thermoacoustic refrigerator. *Therm. Sci. Eng. Prog.* **2024**, *55*, 102938. [CrossRef]
121. Jadhav, S.; Pavitran, S.; Gosavi, S. An energy efficient integration of vapour compression refrigeration with LNG-regasification for freeze desalination applicationsUne intégration écoénergétique du froid par compression de vapeur dans la regazéification du GNL pour les applications de dessalement par congelation. *Int. J. Refrig.* **2023**, *152*, 36–42. [CrossRef]
122. Do Thi, H.T.; Pasztor, T.; Fozer, D.; Manenti, F.; Toth, A.J. Comparison of Desalination Technologies Using Renewable Energy Sources with Life Cycle, PESTLE, and Multi-Criteria Decision Analyses. *Water* **2021**, *13*, 3023. [CrossRef]
123. El Kadi, K.; Adeyemi, I.; Janajreh, I. Application of directional freezing for seawater desalination: Parametric analysis using experimental and computational methods. *Desalination* **2021**, *520*, 115339. [CrossRef]
124. Randall, D.G.; Nathoo, J. A succinct review of the treatment of Reverse Osmosis brines using Freeze Crystallization. *J. Water Process Eng.* **2015**, *8*, 186–194. [CrossRef]

125. Al-Karaghouli, A.; Kazmerski, L.L. Energy consumption and water production cost of conventional and renewable-energy-powered desalination processes. *Renew. Sustain. Energy Rev.* **2013**, *24*, 343–356. [CrossRef]
126. Shahzad, M.W.; Burhan, M.; Ang, L.; Ng, K.C. Energy-water-environment nexus underpinning future desalination sustainability. *Desalination* **2017**, *413*, 52–64. [CrossRef]
127. Rahimnia, R.; Pakizeh, M. Preparation and characterization of PPO/PS porous membrane for desalination via direct contact membrane distillation (DCMD). *J. Membr. Sci.* **2023**, *669*, 121297. [CrossRef]
128. Han, S.; Shin, J.; Rhee, Y.; Kang, S. Enhanced efficiency of salt removal from brine for cyclopentane hydrates by washing, centrifuging, and sweating. *Desalination* **2014**, *354*, 17–22. [CrossRef]
129. Lim, Y.J.; Lai, G.S.; Zhao, Y.; Ma, Y.; Torres, J.; Wang, R. A scalable method to fabricate high-performance biomimetic membranes for seawater desalination: Incorporating pillararene water nanochannels into the polyamide selective layer. *J. Membr. Sci.* **2022**, *661*, 120957. [CrossRef]
130. Orlowska, M.; Havet, M.; Le-Bail, A. Controlled ice nucleation under high voltage DC electrostatic field conditions. *Food Res. Int.* **2009**, *42*, 879–884. [CrossRef]
131. Moon, J.; Kim, D.Y.; Kim, J.H.; Park, K. Cost-based optimization, feasibility study, and sensitivity analysis of forward osmosis/crystallization/reverse osmosis with high-temperature operation for high-salinity seawater desalination. *Desalination* **2024**, *580*, 117531. [CrossRef]
132. Frioui, S.; Oumeddour, R. Investment and production costs of desalination plants by semi-empirical method. *Desalination* **2008**, *223*, 457–463. [CrossRef]
133. Saboori, H. Hybrid renewable energy powered reverse osmosis desalination-minimization and comprehensive analysis of levelized cost of water. *Sustain. Energy Technol. Assess.* **2023**, *56*, 103065. [CrossRef]
134. Sakthivelnathan, N.; Arefi, A.; Lund, C.; Mehrizi-Sani, A.; Muyeen, S.M. Cost-effective reliability level in 100% renewables-based standalone microgrids considering investment and expected energy not served costs. *Energy* **2024**, *311*, 133426. [CrossRef]
135. Blanco-Murillo, F.; Díaz, M.J.; Rodríguez-Rojas, F.; Navarrete, C.; Celis-Plá, P.S.M.; Sánchez-Lizaso, J.L.; Sáez, C.A. A risk assessment on Zostera chilensis, the last relict of marine angiosperms in the South-East Pacific Ocean, due to the development of the desalination industry in Chile. *Sci. Total Environ.* **2023**, *883*, 163538. [CrossRef]
136. Moreira, F.D.S.; Lopes, M.P.C.; de Freitas, M.A.V.; Antunes, A.M.D.S. Future scenarios for the development of the desalination industry in contexts of water scarcity: A Brazilian case study. *Technol. Forecast. Soc. Change* **2021**, *167*, 120727. [CrossRef]
137. Kabir, M.M.; Sabur, G.M.; Akter, M.M.; Nam, S.Y.; Im, K.S.; Tijing, L.; Shon, H.K. Electrodialysis desalination, resource and energy recovery from water industries for a circular economy. *Desalination* **2024**, *569*, 117041. [CrossRef]
138. Xiang, X.; Liu, X. Research on the economic and environmental impacts of China's seawater desalination industry with different technologies in the macroeconomic system. *Desalination* **2022**, *533*, 115734. [CrossRef]
139. Brundage, M.P.; Chang, Q.; Zou, J.; Li, Y.; Arinez, J.; Xiao, G. Energy economics in the manufacturing industry: A return on investment strategy. *Energy* **2015**, *93*, 1426–1435. [CrossRef]
140. Baayyad, I.; Semlali Aouragh Hassani, N.; Bounahmidi, T. Evaluation of the energy consumption of industrial hybrid seawater desalination process combining freezing system and reverse osmosis. *Desalination Water Treat.* **2015**, *56*, 2593–2601. [CrossRef]
141. Zambrano, A.; Ruiz, Y.; Hernández, E.; Raventós, M.; Moreno, F.L. Freeze desalination by the integration of falling film and block freeze-concentration techniques. *Desalination* **2018**, *436*, 56–62. [CrossRef]
142. Lu, K.J.; Cheng, Z.L.; Chang, J.; Luo, L.; Chung, T. Design of zero liquid discharge desalination (ZLDD) systems consisting of freeze desalination, membrane distillation, and crystallization powered by green energies. *Desalination* **2019**, *458*, 66–75. [CrossRef]